OCEAN DRILLING PROGRAM

LEG 167 PRELIMINARY REPORT

CALIFORNIA MARGIN

Dr. Mitchell Lyle
Co-Chief Scientist, Leg 167
CGISS
Boise State University
1910 University Drive
Boise, Idaho 83725
U.S.A.

Dr. Itaru Koizumi
Co-Chief Scientist, Leg 167
Division of Earth and Planetary Sciences
Graduate School of Science
Hokkaido University
Sapporo 060
Japan

Dr. Carl Richter
Staff Scientist, Leg 167
Ocean Drilling Program
Texas A&M University Research Park
1000 Discovery Drive
College Station, TX 77845-9547

Paul J. Fox
Director
Science Operations

Jack Baldauf
Manager
Science Operations

Timothy J.G. Francis
Deputy Director
Science Operations

July 1996

This informal report was prepared from the shipboard files by the scientists who participated in the cruise. The report was assembled under time constraints and is not considered to be a formal publication which incorporates final works or conclusions of the participating scientists. The material contained herein is privileged proprietary information and cannot be used for publication or quotation.

Preliminary Report No. 67

First Printing 1996

Distribution

Electronic copies of this publication may be obtained from the ODP Publications Home Page on the World Wide Web at http://www-odp.tamu.edu/publications.

SCIENTIFIC REPORT

The following scientists were aboard *JOIDES Resolution* for Leg 167 of the Ocean Drilling Program:

Mitch Lyle (Co-Chief Scientist), CGISS, Boise State University, 1910 University Drive, Boise, Idaho 83725, U.S.A., E-mail: mlyle@cgiss.idbsu.edu

Itaru Koizumi (Co-Chief Scientist), Division of Earth and Planetary Sciences, Graduate School of Science, Hokkaido University, Sapporo, 060, Japan, E-mail: itaru@s1.hines.hokudai.ac.jp

Carl Richter (Staff Scientist), Ocean Drilling Program, Texas A&M Research Park, 1000 Discovery Drive, College Station, Texas 77845-9547, U.S.A., E-mail: richter@tamu.edu

Richard J. Behl (Sedimentologist) Department of Geological Sciences, California State University, Long Beach, 1250 Bellflower Boulevard, Long Beach, California 90840-3902, U.S.A., E-mail: behl@csulb.edu

Per Boden, Stockholm University, S-10691 Stockholm, Sweden, E-mail: per.boden@geokem.su.se

Jean-Pierre Caulet (Paleontologist, radiolarians) Laboratoire de Géologie, Museum National d'Histoire Naturelle, 43 rue Buffon, 75005 Paris, France, E-mail: caulet@cimrs1.mnhn.fr

Margaret L. Delaney (Inorganic Geochemist) Institute of Marine Sciences, University of California, Santa Cruz, Santa Cruz, California 95064, U.S.A., E-mail: delaney@cats.ucsc.edu

Peter deMenocal (LDEO Logger) Lamont-Doherty Earth Observatory, Columbia University, Palisades, New York 10964, U.S.A., E-mail: peter@ldeo.columbia.edu

Marc Desmet (Sedimentologist) Institut de Géologie, Université Louis Pasteur, 1 Rue Blessig, F-67084 Strasbourg, France, E-mail: mdesmet@illite.u-strasbg.fr

Eliana Fornaciari (Paleontologist, nannofossils) Dipartimento di Geologia Paleontologia e Geofisica, Università degli Studi di Padova, via Giotto 1, 35137 Padova, Italy, E-mail: eliana@dmp.unipd.it

Akira Hayashida (Paleomagnetist) Department of Geology, University of California, Davis, CA 95616, Email: hayashida@geology.ucdavis.edu. After 1 April 1997: Science and Engineering Research Institute, Doshisha University, Tanabe, Kyoto 610-03, Japan, E-mail: ahay@doshisha.ac.jp

Franz Heider (Paleomagnetist) Institut für Geophysik, Universität München, Theresienstr. 41, 80333 München, Federal Republic of Germany, E-mail: fheider@rockmag.geophysik.uni-muenchen.de

Julie Hood (Physical Properties Specialist) MGG/RSMAS, University of Miami, Miami, Florida 33149-1098, U.S.A., E-mail: hood@kai.rsmas.miami.edu

Steven A. Hovan (Sedimentologist) Geoscience Department, Indiana University of Pennsylvania, 114 Walsh Hall, Indiana, Pennsylvania 15705-1087, U.S.A., E-mail: hovan@grove.iup.edu

Thomas R. Janecek (Stratigraphic Correlator) Antarctic Marine Geology Research Facility, Florida State University, Antarctic Research Facility, Tallahassee, Florida 32306-3026, U.S.A., E-mail: janecek@gly.fsu.edu

Aleksandra G. Janik (Physical Properties Specialist) RSMAS-MGG, University of Miami, 4600 Rickenbacker Causeway, Miami, Florida 33149-1098, U.S.A., E-mail: alek@kai.rsmas.miami.edu

James Kennett (Paleontologist, foraminifers) Director, Marine Science Institute, University of California, Santa Barbara, Santa Barbara, California 93106, U.S.A., E-mail: kennett@msi.ucsb.edu

David Lund (Physical Properties Specialist) College of Oceanic and Atmospheric Sciences, Oregon State University, Oceanography Admin. Bldg. 104, Corvallis, Oregon 97331-5503, U.S.A., E-mail: dlund@oce.orst.edu

Maria L. Machain Castillo ((Mexican Observer; Paleontologist, foraminifers/ostracods) Institute de Ciencias del Mar y, Limnologia, Universidad Nacional Autónoma de Mexico, Apdo. Postal 70-310, Mexico 04510, D.F., Mexico, Email: machain@mar.icmyl.unam.mx

Toshiaki Maruyama (Paleontologist, diatoms) Department of Earth Sciences, General Education Building, Yamagata University, Kojirakawa, Yamagata 990, Japan

Russell Merrill (Physical Properties Specialist, Digital Imaging) Ocean Drilling Program, Texas A&M Research Park, 1000 Discovery Drive, College Station, Texas 77845-9547, U.S.A., E-mail: Russell_Merrill@odp.tamu.edu

David J. Mossman (Sedimentologist) Department of Physics, Engineering and Geology, Mount Allison University, Sackville, New Brunswick E0A 3CO, Canada, E-mail: dmossman@mta.ca

Jennifer Pike (Sedimentologist) Department of Oceanography, University of Southampton, Southampton Oceanography Centre, European Way, Southampton SO14 3ZH, United Kingdom, E-mail: jp@soton.ac.uk

A. Christina Ravelo (JOIDES Logging Scientist/Stratigraphic Correlator) Institute of Marine Sciences, University of California, Santa Cruz, Santa Cruz, California 95064, U.S.A, E-mail: acr@aphrodite.ucsc.edu

Gloria A. Rozo Vera (Mexican Observer; Paleontologist, foraminifers) CICTUS/Universidad De Sonora, Rosales y Niños Heroes S/N, A.P. 1819, C.P. 83000, Hermosillo, Sonora, Mexico, Email: grozo@guaymas.uson.mx

Rainer Stax (Organic Geochemist) Institute for Geology & Mineralogy, University of Erlangen, Schlossgarten 5, 91054 Erlangen, Federal Republic of Germany, E-mail: rstax@geol.uni-erlangen.de

Ryuji Tada (Sedimentologist) Geological Institute, University of Tokyo, 7-3-1 Hongo, Bunko-ku, Tokyo 113, Japan, E-mail: ryuji@geol.s.u-tokyo.ac.jp

Jürgen Thurow (Sedimentologist/Digital Imaging) Department of Geological Sciences, University College London, Gower Street, London WC1E 6BT, United Kingdom, E-mail:j.thurow@ucl.ac.uk

Masanobu Yamamoto (Organic Geochemist) Fuel Resources Department, Geological Survey of Japan, 1-1-3 Higashi, Tsukuba, Ibaraki 305, Japan, E-mail: yamamoto@gsj.go.jp

ABSTRACT

The main objectives for drilling Leg 167 were to investigate the evolution of oceanogaphic conditions in the North Pacific Ocean and to document changes in flow of the California Current system and associated changes in coastal upwelling. These data will be used to reconstruct North Pacific climate conditions through the Neogene, concentrating upon the time period since the advent of Northern Hemisphere glaciation, about 2.5 Ma to the present. Four of the drill sites (Sites 1010, 1011, 1014, and 1016) sampled middle to upper Miocene sediments to reconstruct a Neogene history of the California Current. The results of Leg 167 drilling will also be used to better understand the links between climates of the North Pacific Ocean and western North America, particularly in terms of temperature change and changes in precipitation.

The 13 sites are organized into three transects across the California Current (Baja Transect, ~30°N; Conception Transect, ~35°N; and Gorda Transect, ~40°N) and one coastal transect extending from northern Baja California to the California/Oregon border, 30°N to 42°N. Each of the three transects across the California Current compares deep-water sites near the core of the California Current to coastal upwelling sites near shore. The coastal transect examined variations in upwelling and productivity along the California Margin, and also intermediate-water properties in many of the basins of the California Continental Borderland.

INTRODUCTION

The California Current system is probably the best investigated eastern boundary current system in the world, with well-known physical dynamics, chemical structure, biological standing stocks, and biogeochemical fluxes. Nevertheless, the response of the California Current system and associated coastal upwelling systems to climate change is poorly documented. Climate models and available paleoceanographic data indicate that the California Current system changed dramatically with the growth and decay of the North American ice sheets. The paleoceanographic records, however, remain too sketchy to test the models.

Ocean Drilling Program (ODP) Leg 167 (Fig. 1) represents the first time since 1978 that the Pacific margin of North America was drilled to study ocean history. The leg collected both high-resolution records appropriate for studying events with durations of a few thousand years or less within the Pleistocene and Pliocene and lower-resolution records to examine much of the Neogene interval. Sites were drilled to collect sediments needed to study the links between the evolution of North Pacific climate and the development of the California Current system. The same material will also be used to study the climate links between the North Pacific Ocean and North America.

Only three other drilling legs, all part of the Deep Sea Drilling Project (DSDP), have sampled the historical sediment record along the California Margin. A single advanced hydraulic piston core (APC) site in the Santa Barbara Basin (Site 893) represents all of ODP drilling before Leg 167. The last major drilling effort, DSDP Leg 63, occurred immediately before the first deployment of the APC. Recovered core from the DSDP drilling is discontinuous and very disturbed, so it is impossible to use this material for modern, high-resolution, paleoceanographic studies. Reconnaissance studies using DSDP cores have shown, however, that the Leg 167 drilling region is highly sensitive to climate change and that new ODP drilling would collect a detailed record of this variability.

Significant contrasts in sedimentary environments occur along the California Margin, including the unique tectonic and sedimentary environments of the basins in the California Borderland. Site selection exploited these opportunities, constructing latitudinal, longitudinal, and depth transects. There are three east-west transects, with at least two sites in each transect, one located in the coastal upwelling zone (from 50 to 90 km offshore, 1000 to 2000 m water depth) and one in the core of the California Current proper (from 150 to 360 km offshore, 3500 to 4200 m water depth). The **Gorda Transect** (~40°N; Sites 1019, 1022, 1020, and 1021) is in a region of strong summer upwelling. The **Conception Transect** (~35°N; Sites 1017 and 1016) is influenced by year round upwelling with relatively cool surface waters. The **Baja Transect** (~30°N; Sites 1011 and 1010) is influenced by year-round upwelling with warmer surface waters. The oldest sediments from the inshore sites are Pleistocene in age, and from the offshore sites, middle or late Miocene. Coastal upwelling processes at the margin will be reflected in the nearshore sites, whereas nutrient supply by California Current processes will be reflected in the deeper sites.

The north-south **Coastal Transect** covers the latitude range from 31° to 42°N (in order from north to south: Sites 1019, 1022, 1018, 1017, 1014, 1013, 1012, and 1011). All sites are within <160 km offshore, in water depths of 1000–2500 m. The oldest sediments from all sites are at least Pleistocene in age, and some range to late Miocene. The coastal transect will detail the history of coastal upwelling and of continent-ocean interaction.

Sites also constitute two depth transects. The **Northern Depth Transect** (~37° to 42°N, from 60 to 360 km offshore; Sites 1019, 1022, 1018, 1020, and 1021) covers 1000–4200 m water depth. Oldest sediments from Site 1019 are Pleistocene, whereas the sediments from the deepest-water site (Site 1022) range in age from latest middle Miocene to Quaternary in age. The **Southern Depth Transect** (~30° to 35°N, from 30 to 210 km offshore; Sites 893 [Leg 146], 1015, 1017, 1013, 1014, 1012, 1011, 1010, and 1016) covers 475–3850 m water depth. This transect takes advantage of the different sill depths within the California Borderlands for detailed study of the shallow intermediate water column. The oldest sedi-

ments from sites with the shallower water depths are at least late Pleistocene in age, whereas basal sediments from the sites with deeper water depths are typically late Miocene. These depth transects will provide sediments to investigate hypotheses about water-depth control of sedimentation processes and water column structure and its evolution through time.

EXPECTED SCIENTIFIC RESULTS FROM LEG 167

The response of California Current structure and hydrography to insolation forcing and Northern Hemisphere glaciation will be defined by Leg 167 studies, as will the longer-term oceanographic evolution of the northeastern Pacific. The sediments collected on Leg 167 will provide one of the first direct opportunities to quantify the linkages between tropical and polar climates over a broad spectrum of age scales. The Neogene histories of biogenic carbonate and opal accumulation at these drill sites will constrain their basinal and global distributions. Results from the depth transect sites will shed light on questions about deep-water hydrography, such as the existence and significance of Pacific intermediate- or deep-water formation and the linkages between deep Atlantic and Pacific circulation and carbonate burial. Significant advances in the understanding of regional biostratigraphy, of the origin of physical property variations, of rock magnetic properties, and of lithologic cyclicity will result as well. Modeling, ranging from simple box models to coupled ocean/atmosphere models, will complement data interpretation. Diagenesis of organic matter and inorganic components in sediments will be much better understood from the study of pore-water and solid-phase composition from the variety of different environments drilled during Leg 167.

Site 1010 (Proposed Site CA-14A)

One of the primary objectives of Site 1010 (Fig. 1) was to provide chronological control for

biostratigraphic events in the California Current region through the middle Miocene. Because subtropic and subarctic flora and fauna mix along the coast of California, the detailed biostratigraphy fits imperfectly with schema developed for either the tropics or the subarctic North Pacific. A second important goal is the Neogene paleoceanography of the southern region of the California Current. In the modern oceans, the California Current can be distinguished by its temperature and salinity characteristics to the southern tip of Baja California. Site 1010 provides a means to monitor this southern region because it is located underneath the approximate core of the current. Site 1010 will also be used to study organic matter diagenesis. In addition, high-resolution stable isotope profiles of intersitial water will be used to study ice volume at the last glacial maximum. A secondary goal was to obtain a representative sample of the basaltic basement for igneous petrology and geochemistry.

The sedimentary sequence at Site 1010 (Fig. 2) consists of an apparently continuous, 185-m-thick interval of Quaternary to middle Miocene sediments. They are divided into four lithologic units. Unit I (0–18.5 meters below seafloor [mbsf]) consists of siliciclastic sediments (silty clays and clayey silts) with abundant vitric ash layers and disseminated volcanic glass throughout. The top of Unit II (18.5–66.0 mbsf) is defined by increased biogeneous sediment components and consists of interbedded units alternating between nannofossil ooze and silty clay. Volcanic ash layers (both vitric volcanic ash and altered) are abundant. Unit III (66.0–178.0 mbsf) represents increased siliceous components interbedded throughout with clay and nannofossil sediments. Interbedding occurs on a scale of 20–80 cm. Unit IV (178.0–basement) is composed of alternating porcellanite, nannofossil chalk, and clay. The tagged basement consists of basalt.

Core-core correlation between the 5 holes successfully established a continuous composite record down to 110 mbsf. More detailed work is in progress for cores below this depth. Scatter in bulk density values determined from discrete sediment samples matches the bulk densities obtained using the gamma-ray attenuation porosity evaluator (GRAPE) well. Ve-

locities increase slowly downhole with very slight variation. High velocities correspond to low porosity values.

The section includes an upper 60-m-thick sequence containing variable but often abundant planktonic foraminifers and few diatoms, radiolarians, and calcareous nannofossils from the Quaternary through the lowermost Pliocene and uppermost Miocene (Fig. 2). This is underlain by a 70-m-thick sequence of late Miocene to late middle Miocene age marked by an almost complete absence of planktonic foraminifers and generally uncommon calcareous nannofossils, diatoms, and radiolarians. This is underlain by a 55-m-thick sequence of rapidly deposited diatom ooze of middle middle Miocene age (base: diatom *Denticulopsis hyalina* Zone, 13.1–13.9 Ma; Nannofossil Zone CN4, 13.6 to 15.8 Ma). These diatom oozes contain assemblages of diatoms, radiolarians, and planktonic foraminifers indicative of extensive upwelling of cool waters associated with the California Current. The radiolarian assemblages are the best-preserved Miocene examples from an intense upwelling province, and include numerous new species never observed before. Likewise, the planktonic foraminifer assemblages provide a rare insight into the characteristics of faunas associated with intense Miocene upwelling. The sequence of changes in planktonic foraminifers suggests the need to establish a new zonation for the southern California Current system.

A complete magnetostratigraphy was determined from Holes 1010C and 1010E (Fig. 2). All chrons from the Brunhes to the top of Chron C3Bn (7 Ma) could be identified in the upper 75 mbsf. The age-depth plot based on magnetic reversals shows three linear segments, representing 3 different sedimentation rates in the upper 75 mbsf. Below 75 mbsf, the intensity of magnetization decreases. The drilling-induced remanent magnetization dominates between 75 and 160 mbsf and prevents the identification of polarity reversals.

No significant amounts of gas were measured in the sediment column. Carbonate contents vary strongly between 0 and 80 wt% in the upper 110 mbsf. Below this depth, carbonate contents are generally higher than the upper section because of higher nannofossil concen-

tration. Organic carbon values decrease with depth from about 0.4 to less than 0.2 wt%.

Interstitial water samples for shipboard analysis were taken 1 per core for the first 10 cores and then 1 every third core to about 170 mbsf. A high-resolution suite of samples was also taken from one hole at 1/section spacing (about 1.5 m) for shorebased study. The interstitial water geochemistry is typical of an open ocean site, showing the influence of reactions in the underlying basalt via diffusion, of the relatively low organic carbon content of the sediments, and of the dissolution of biogenic silica. Chloride increases slightly with increasing depth, from 559 to 569 mM at around 80 mbsf, then decreases again. Calcium increases with increasing depth, with an average gradient of 4.2 mM/m, and magnesium decreases with increasing depth, with an average gradient of –3.3 mM/m. Calcium and magnesium are linearly correlated with each other. Alkalinity increases only slightly to values over 4 mM at depths of 20–60 mbsf. Sulfate indicates a minor amount of organic carbon oxidation via sulfate reduction, with values between 24 and 29 mM throughout the section. Phosphate has elevated values around 6 μM in the upper 10 m, with values between 2 and 3 μM at greater depth. Ammonia increases with depth to values around 130 mM. Silicate increases with increasing depth to values greater than 1000 μM by 75 mbsf.

Site 1011 (Proposed Site CAM-2A)

Site 1011 is the landward site of the Baja Transect, which crosses the California Current at about 30°N (Fig. 1). Site 1011 was drilled to study both surface-water properties and water-column structure for the upper Miocene to Quaternary interval. It was also drilled to sample a sedimentary section to acoustic basement to determine the nature of the basement and to gather information on the opening and subsidence of Animal Basin.

The sedimentary sequence at Site 1011 consists of an apparently continuous, 281.5-m-thick interval of Quaternary to upper Miocene sediments. They are divided into four lithologic units. Unit I (0.0–25.0 mbsf) consists of upper Quaternary (0.0–1.0 Ma) siliclastic sedi-

ments, predominantly clays and silt, with vitric ash layers and graded quartz sand beds. Unit II (25–204 mbsf) is characterized by an increase in calcium carbonate and consists of upper Miocene to Quaternary (1.0–7.9 Ma) interbedded silty clay and nannofossil ooze on a decimeter to meter scale. Volcanic ash layers occur above 118 mbsf and below 184 mbsf. Graded sand beds occur above 98 mbsf. This unit is divided into three subunits. Subunit IIA consists of interbedded nannofossil ooze and silty clay. Subunit IIB is defined by a marked decrease in calcareous nannofossil content and increase in silty clay. Subunit IIC reflects an increase in lithification and in calcareous nannofossils. In Unit III (204–262 mbsf) the dominant biogenic component changes from calcareous nannofossils to siliceous microfossils. Subunit IIIA consists of upper Miocene (7.9–9.2 Ma) interbedded clayey diatomites and nannofossil diatomites. Subunit IIIB is defined by a lithologic change to almost pure diatomites (9.4–9.5 Ma). Unit IV (262–276 mbsf) was poorly recovered and consists of indurated siltstone and sandstone. Basement was reached at 276 mbsf and recovered 1.89 m of fine-grained vesicular basalt.

Detailed comparisons between the magnetic susceptibility and GRAPE density records generated using the multisensor track (MST), and high-resolution color reflectance measured using the Oregon State University system, demonstrated complete recovery of the sedimentary sequence down to 150 mbsf.

The section includes an upper 132-m-thick sequence containing abundant planktonic foraminifers, calcareous nannofossils, few benthic foraminifers, and rare to absent diatoms and radiolarians from the late early Pliocene to the Quaternary (Fig. 3). This is underlain by a 48-m-thick sequence of late late Miocene to early Pliocene age characterized by rare and sporadic assemblages of planktonic foraminifers, few to abundant calcareous nannofossils, and generally uncommon diatoms and radiolarians. Below this interval, a 110-m-thick sequence of rapidly deposited diatom-rich sediments of late Miocene age was recovered. These sediments contain abundant diatoms and radiolarians. Calcareous nannofossils and planktonic foraminifers are rare or absent. Benthic foraminifers assemblages are less con-

sistently present. The base of the sedimentary sequence is assigned to the middle late Miocene diatom *Denticulopsis dimorpha* Zone, indicating an age of approximately 9 Ma.

Dominant cold species of planktonic foraminifer, diatom, and radiolarian assemblages exhibit evidence of strong upwelling conditions during the late Miocene. Domination of temperate foraminiferal species in early late Pliocene through early Pleistocene assemblages, and rare occurrences of diatoms and radiolarians, indicate warm temperate to cool subtropical conditions with a weakening of the upwelling system. The late Pliocene to Quaternary planktonic foraminiferal assemblages indicate cooler conditions with major sea-surface temperature changes related to glacial-interglacial episodes. Fewer occurrences of subtropical forms suggest generally cooler conditions than during the early and early late Pliocene.

A magnetostratigraphy could not be obtained. An interesting feature of the paleomagnetic data at this site is the steplike reduction of magnetic intensity between 1.5 and 2.5 mbsf. The intensity drop corresponds to the decrease in magnetic susceptibility in the same interval because of a strong decrease in concentration of magnetic minerals within 1 m. Dissolution of fine magnetic minerals is caused by diagenetic sulfate reduction in these highly organic sediments.

Significant amounts of biogenic methane gas were observed. Headspace methane concentration increased with increasing depth and reached a maximum (6347 ppm) at 89 mbsf and a high concentration (2505 ppm) at around 190 mbsf. No significant higher weight molecular hydrocarbons were observed, indicating that the methane is of biogenic origin and not significant for safety and pollution investigations. The carbonate content varies strongly between 1 and 73 wt%, and is generally high in lithostratigraphic Unit IIA. The organic carbon contents is high (0.3%–6.6%) throughout the section. The correlation between organic carbon and the C to N ratio suggests a predominantly terrigenous origin of to the organic material.

Chemical gradients in the interstitial waters (Fig. 4) reflect organic matter diagenesis via sulfate reduction, an increase in dissolved sulfate at greater depth, the dissolution of biogenic opal, and the influence of authigenic mineral precipitation. The decrease in dissolved calcium in the upper sediment, coincident with the sulfate decrease and the alkalinity increase from sulfate reduction, and the nonlinear relationship of calcium and magnesium suggest that authigenic mineral precipitation is significant in influencing the geochemical profiles.

Porosity decreases with depth in the upper 150 mbsf and shows an inverse correlation with *P*-wave logger (PWL) velocity. The lowest porosity values (55%) were measured in a very clay-rich interval (140–150 mbsf). Porosity increases slightly from 55% to 70% below 150 mbsf. At about 204 mbsf, the grain density values drop from around 2.7 to 2.5 g/cm^3, reflecting the transition from clay-rich sediments with well-preserved calcareous nannofossils to siliceous sediments, marking the boundary between lithostratigraphic Units II and III.

Color reflectance data allowed for real-time prediction of sedimentary opal content. Using a regression equation generated from site-survey reflectance and opal measurements, we were able to simulate major lithologic units. Low opal content coincided with lithostratigraphic Units I and II, which included silty clay, and nannofossil ooze and chalk. Opal maxima and minima corresponded to interbedded diatomite and clay of lithostratigraphic Unit IIIA. The highest predicted opal content matched Unit IIIB, a diatomite. Opal levels were low in the siltstone, silty clay, and sandstone of Unit IV.

Core images were captured using the ODP color digital imaging system. Colors were measured and reported in the CIELAB system and appear to correlate with GRAPE density, possibly reflecting the carbonate component.

Logging at Hole 1011B consisted of two full passes with the Triple Combination tool string

(density, neutron porosity, resistivity, and natural gamma ray) and one full pass with the Formation MicroScanner-Sonic (FMS-Sonic) tool string. Hole conditions were excellent, so the recorded log data were of excellent quality. The log physical property data closely matched the measured core density and porosity over the core-log data overlap; the log sonic velocity data were unfortunately not reliable because of the very high porosity sediments and consequent low impedance contrast. The log variations clearly delineate the major and minor lithologic boundaries. A sharp reversal to higher porosities below 200 mbsf is caused by an upper Miocene diatomite interval; this lithologic boundary represents a strong seismic reflector that may be useful for regional correlations. The FMS data revealed clear carbonate-clay interbedding that can be matched with the core MST data, particularly over the high sedimentation rate section below 200 mbsf.

Site 1012 (Proposed Site BA-1)

Site 1012 is located in East Cortez Basin, within the middle band California Borderland basins in a water depth of 1783 m (Fig. 1). The primary objective was to sample a high-resolution section from the early Pliocene to Quaternary to study the evolution of the California Current system and oceanographic processes in intermediate waters as Northern Hemisphere glaciations expanded. Paleoceanographic proxies for surface-water properties will be sampled at a high resolution, including those for sea-surface temperature, paleoproductivity, and water mass. The site will also be important for high-resolution paleomagnetic studies and will provide important new information about organic carbon diagenesis and about minor-element geochemistry through pore-water profiles.

The sedimentary sequence recovered at Site 1012 consist of an apparently continuous, 264-m-thick interval of upper lower Pliocene to Quaternary sediments. It consists of a single lithologic unit with two subunits. Lithologic Unit I consists of interbedded silty clay, nannofossil mixed sediment, and nannofossil ooze, and their lithified equivalents. The sedi-

ments are organic-rich throughout, and cyclic variation in organic matter content is superimposed upon the carbonate/siliciclastic cycles. Subunit IA is composed of silty clay, nannofossil mixed sediment, and nannofossil ooze. Mean carbonate composition increases downcore from 15% to 50%. Subunit IB is composed of silty clay, and lithified clayey nannofossil mixed sediment and nannofossil chalk, along with isolated beds of dolostone. Mean carbonate values remain approximately at 50%, although bed-to-bed variation is great. Dolostone beds and the presence of glauconite are associated with an upper Miocene to upper lower Pliocene hiatus or condensed interval at the base of the sequence.

Detailed comparisons between the magnetic susceptibility record generated using the MST, and high-resolution color reflectance measured using the Oregon State University system, demonstrated complete recovery of the sedimentary sequence down to 94 mbsf. The correlation between carbonate content and bulk density is excellent. The scatter reflects the alternating carbonate-rich and carbonate-poor layers. Downhole temperature measurements yield a thermal gradient of 82°C/km. Using an average thermal conductivity of 0.905 W/(m·K) provides a heat-flow estimate of 74 mW/m^2.

Uppermost Miocene planktonic foraminifers (5.6 to 6.2 Ma) at the bottom of Hole 1012A suggest that much of the lower Pliocene is missing at Site 1012 or that there is a highly condensed lower Pliocene sequence. Calcareous nannofossils are abundant and well preserved in the Quaternary and upper Pliocene, and poorly preserved and fragmented in the upper lower Pliocene and uppermost Miocene. Planktonic foraminifers are highly abundant and very well preserved in the Quaternary, abundant to common and generally well preserved throughout the Pliocene, and are few but well preserved in the uppermost Miocene. Radiolarians and diatoms are absent in the sequence except for conspicuous reworked middle Miocene species.

A well-constrained biostratigraphy and chronology is provided by calcareous nannofossils and planktonic foraminifer datums for the upper Pliocene and Quaternary. Extensive re-

working of calcareous nannofossils in the upper lower Pliocene and uppermost Miocene made biostratigaphic determinations more difficult based on calcareous nannofossils. Lower upper Pliocene microfossil assemblages indicate relatively warm-temperate conditions, which change in the latest Pliocene to Quaternary to cooler conditions with major sea-surface temperature changes related to glacial/interglacial oscillations.

Paleomagnetic alternating field (AF) demagnetization at 20 mT revealed an excellent magnetostratigraphic record between 0 and 130 mbsf. The Brunhes (C1n), the Jaramillo (C1r.1n), Cobb Mountain, and the Olduvai (C2n) normal polarity intervals were identified. An age-depth plot based on the reversal boundaries gives a constant sedimentation rate of 65 m/m.y.

The calcium carbonate record is characterized by a very high fluctuation of values, ranging from 5 to about 70 wt%. The carbonate concentration increases steadily downcore to 120 mbsf and reaches constant values around 50 wt%. Organic carbon contents are high throughout the sediment column and dominated by marine organic matter according to low C to N ratios. Episodic input of terrigenous organic matter leads to increased organic carbon values. Volatile hydrocarbons are consistently very high, but are of no safety or pollution concern because of high C1 to C2 ratios.

The interstitial water geochemistry (Fig. 4) reflects the influence of organic carbon diagenesis by sulfate reduction, of biogenic opal dissolution, and of possible authigenic mineralization reactions. Dissolved sulfate reaches concentrations <1 mM by 18 mbsf. Alkalinity increases to as high as 60 mM, dissolved phosphate to 120 μM, and ammonium to 14 mM. Opal dissolution is indicated by the increase of dissolved silicate to values >1000 μM by 130 mbsf. Nonconservative profiles of calcium and magnesium suggest the importance of authigenic mineralization.

A multiple linear regression was used to construct an empirical relationship between calci-

um carbonate and reflectance measurements gathered at Site 1011. Using this regression equation, carbonate content was predicted at Site 1012. The predicted values matched laboratory data well. Fluctuations are highly cyclic—preliminary spectral analysis of reflectance data in a crude age model framework show power in the Milankovitch frequencies. The high-resolution reflectance data imply calcite variations not resolved by the lower resolution carbonate samples.

Site 1013 (Proposed Site BA-2B)

Site 1013 is located in San Nicolas Basin, within the middle band of basins of the California Borderlands in water depth of 1575 m (Fig. 1). The primary objective of drilling at this site was to sample a high-resolution section from the early Pliocene to Quaternary to study the evolution of the California Current system and to study oceanographic processes in intermediate waters as Northern Hemisphere glaciations expanded. Site 1013 will also provide information about organic carbon diagenesis and about minor-element geochemistry through pore-water profiles and through solid-phase analyses. Because of its location, away from the turbidites that fill the inner Borderland basins, we expect most of the organic matter in the basin to be marine in origin.

The sedimentary sequence recovered from the three holes at Site 1013 consists of an apparently continuous, 146-m-thick interval of upper upper Pliocene (2.7 Ma) through Quaternary sediments. Sediments gradually change from mixtures of siliciclastic and biogenic components to mixtures of biogenic and minor siliciclastic components. Interbedding of the sediments is on a scale of less than a meter to several meters. Siliciclastic clay and silt are found throughout the cored interval, but strongly decrease downhole. Calcareous nannofossils and to a lesser extent foraminifers strongly increase downhole, and dominate the calcareous fraction of the sediments. The biosiliceous component is negligible. Thin terrigenous siliciclastic sand layers occur in the upper part of the sequence and distinct ash layers

throughout the lower part of the sequence.

Detailed comparisons between the magnetic susceptibility record generated using the MST, and high-resolution color reflectance measured using the Oregon State University system, demonstrated complete recovery of the sedimentary sequence down to 97 mbsf.

Calcareous nannofossils are abundant throughout and preservation is moderate to good. Planktonic foraminifers are abundant and well preserved in the Quaternary, and abundant to rare and moderately well preserved in the uppermost Pliocene. Radiolarians and diatoms are absent in the sequence except for conspicuous reworking of middle Miocene species. Reworked calcareous nannofossils of middle Miocene and Eocene age occur in the Quaternary. A well-constrained biostratigraphy and chronology is provided by calcareous nannofossil and planktonic foraminifer datums for the upper part of the Pliocene and Quaternary.

Latest Pliocene through Quaternary planktonic foraminifer assemblages indicate large-scale oscillations in sea-surface temperatures associated with glacial/interglacial episodes. Benthic foraminifer assemblages suggest relatively low oxygen concentrations in the basin during the late Neogene. Near suboxic to suboxic basinal conditions occurred during the latest Pliocene to earliest Quaternary.

AF demagnetization at 20 and 25 mT revealed a complete magnetostratigraphic record between 0 and 95 mbsf. The Brunhes (C1n), the Jaramillo (C1r.1n), possibly the Cobb Mountain, and the top of the Olduvai (C2n) normal polarity intervals were identified. An age-depth plot based on the reversal boundaries gave a sedimentation rate of 65 m/m.y around the Jaramillo and a lower sedimentation rate below the Cobb Mountain.

Headspace volatile hydrocarbons rapidly increase at about 20 mbsf and stay consistently high throughout the sedimentary column. Methane to ethane ratios, however, are in the normal range of biogenic methanogenesis. The calcium carbonate record from 0 to 50 mbsf

shows slightly increasing values between 5 and 30 wt% with a low fluctuation. Below 50 mbsf, the fluctuation increases to about 40 wt%, and highest values occur in the deepest part of the hole. Organic carbon ranges from 1 to 6 wt% (to a maximum of 9 wt%). The ratios of organic carbon to total nitrogen range from 8 to 12, indicating a marine provenance of the organic matter at this site.

The interstitial water geochemistry (Fig. 4) reflects the influence of organic carbon diagenesis by sulfate reduction, of biogenic opal dissolution, and of possible authigenic mineralization reactions. Dissolved sulfate reaches concentrations <1 mM by 19 mbsf. Alkalinity increases to as high as 60 mM, dissolved phosphate to 150 μM, and ammonium to 13 mM. Opal dissolution is indicated by the increase of dissolved silicate to values >1000 μM by 76 mbsf. Nonconservative profiles of calcium and magnesium suggest the importance of authigenic mineralization.

Physical properties show very little variation downhole corresponding to the sedimentological findings. The few variations most likely correspond to fluctuating amounts of clay and carbonate. Three downhole temperature measurements were taken using the Adara tool, and gave a geothermal gradient of 72°C/km (Fig. 5). The heat-flow estimate at Site 1013 is 65 mW/m^2.

The ODP Digital Color Video images correlate very well with those obtained using the Oregon State University Color Reflectance tool. Additionally, there appears to be a relationship between color and discrete index properties, in particular, density. This is probably a result of the color variations associated with carbonate concentration, and the strong correlation between density and carbonate content. Reflectance data were used to predict high-resolution carbonate concentrations in real time.

Site 1014 (Proposed Site CA-15A)

Site 1014 is located in Tanner Basin, within the outer band of California Borderland basins (Fig. 1). The primary objective was to sample a high-resolution section from the late Miocene to Quaternary to study the evolution of the California Current system and to study oceanographic processes in intermediate waters as Northern Hemisphere glaciations expanded. The site will also provide important information about organic carbon diagenesis and about minor-element geochemistry through pore-water profiles and through solid-phase analyses. Pore-water sampling especially within the upper 100 m will be used to define the rates of organic matter oxidation and the removal of oxidants from the pore waters and sediments, whereas organic geochemical analysis will provide data on organic matter preservation in a low oxygen environment.

The sedimentary sequence recovered from the 4 holes at Site 1014 consists of a well-dated, apparently continuous, 325-m-thick interval of upper Pliocene to Quaternary sediments, underlain by a relatively poorly dated, 124-m-thick sequence of early Pliocene to possible latest Miocene age.

The sediments are homogeneous throughout the entire sequence, and consist dominantly of calcareous nannofossils and foraminifers and siliciclastic clays. The sequence is divided into two lithologic subunits. Subunit IA (0–140 mbsf) contains interbedded clay with foraminifers and nannofossil ooze with foraminifers and clay. Subunit IB (140–449 mbsf) contains an increased amount of calcareous nannofossils, and is composed of nannofossil ooze and nannofossil chalk alternating with clay-rich intervals. Discrete ash layers and thin dolostone beds occur in the lower part of the sequence.

Detailed comparisons between the magnetic susceptibility record generated using the MST, and high-resolution color reflectance measured using the Oregon State University system, demonstrated complete recovery of the sedimentary sequence down to 160 mbsf.

Biostratigraphic age control was provided by a combination of calcareous nannofossil, planktonic foraminifer, and radiolarian datums for the upper Pliocene and Quaternary. The base of the sequence is not well dated, but calcareous nannofossils suggest a late Miocene age of between 5 and 7 Ma.

Diatom and radiolarian assemblages suggest weak to strong upwelling cycles during the late Pliocene leading to high-productivity episodes on the continental margin. Middle to upper Miocene diatom and radiolarian species suggest a persistent input of reworked material throughout this sequence. Planktonic foraminifer and radiolarian assemblages indicate relative warmth from the early Pliocene through the late Pliocene until 2.5 Ma. Cooling at thermocline depths is suggested after 3.0 Ma by cooler radiolarian assemblages. This was followed at 2.5 Ma by a major surface-water cooling. Low oxygen concentrations in basinal bottom waters during the earliest Quaternary through latest Pliocene coincided with strong upwelling conditions. During the Quaternary, benthic foraminifer assemblages change in association with glacial-interglacial oscillations. This suggests changes in upper intermediate water circulation during late Quaternary climatic cycles.

AF demagnetization at 20 mT revealed a good magnetostratigraphic record between 0 and 100 mbsf. The Brunhes (C1n) and the Jaramillo (C1r.1n) normal polarity intervals were identified. An age-depth plot based on the reversal boundaries gives a constant sedimentation rate of 79 m/m.y. for the past 2.6 m.y.

Methane to ethane ratios determined from vacutainer and headspace samples are high throughout the sediment column. Average values of calcium carbonate contents steadily increase from 30 wt% at the top of the core to about 55 wt% at 250 mbsf and decrease again at the bottom. The pattern show a high-amplitude fluctuation ranging from 20 to 35 wt%. Organic carbon values are very high (2 to 9 wt%). According to low C to N ratios, the organic material is mainly of marine origin.

The interstitial water geochemistry (Fig. 4) reflects the influence of organic carbon diagenesis by sulfate reduction, of biogenic opal dissolution, and of possible authigenic mineralization reactions. Dissolved sulfate reaches concentrations <1 mM by 17.05 mbsf. Alkalinity increases to values >100 mM, dissolved phosphate to >200 µM, and ammonium to 40 mM. Opal dissolution is indicated by the increase of dissolved silicate to values >1000 µM by 136.6 mbsf. Nonconservative profiles of calcium and magnesium indicate the potential importance of authigenic mineralization.

Index properties show a rapid increase in density and associated decreases in void ratio, porosity, and water content to about 50 mbsf, where coring was switched from the APC to the extended core barrel (XCB) system. Below this depth, the downhole physical property changes are slow, with few fluctuations, most likely corresponding to changing amounts of clay and carbonate. However, at approximately 140 mbsf, densities shift to higher values, whereas void ratio, porosity, and water content values drop. At this depth an increase in carbonate content occurs and is marked as the change from lithologic Unit IA to IB.

Thermal conductivity is low, 0.842 W/(m·K) on average, and provides a heat-flow estimate of 49 mW/m^2 (Fig. 5).

Color reflectance data were used to predict high-resolution carbonate measurements aboard ship. Two separate regression equations were used, one based on Site 1012 reflectance and carbonate data and the other based on a combined data set from Sites 1012 and 1013. The combined equation was an effort to compensate for the effect of high organic carbon content at Site 1014. Carbonate content was simulated well by both equations, generally matching the laboratory measurements in both amplitude and phase.

Logging was conducted at Hole 1014A from the base of pipe set at 80 mbsf to a sub-bottom depth of 445 mbsf. Hole conditions were excellent, with the exception of a few washouts.

The log physical property data closely matched the measured core density, porosity, and susceptibilty (Fig. 6) over the core-log data overlap.

The log gamma-ray values exhibit very high values between 100 and 160 mbsf. The gamma-ray activity throughout the hole is predominantly caused by variations in the uranium content, which is strongly correlated to measured variations in sediment organic carbon content. The uranium-organic carbon linkage appears to reflect authigenic uranium fixation in these strongly reduced sediments. High sedimentation rates at Site 1014 provide an opportunity to examine the core and log resolution of orbital and millennial-scale bedding cycles (Fig. 6). Comparison of the FMS record (averaged to 2 mm resolution) with the digital video brightness (L*) channel data (decimated to 4 mm resolution) suggests that periodic variability in carbonate composition at the 20–30 cm scale (equivalent to 2–3 k.y.) can be faithfully resolved in the log data.

Site 1015 (Proposed Site BA-4D)

Site 1015 is located in Santa Monica Basin in water depth of 912 meters below sea level (mbsl) (Fig. 1). It is the only Leg 167 drill site within an inner borderland basin. This basin goes periodically anoxic, because the source of deep water is very near the oxygen minimum. Distal turbidites from the Hueneme Fan extend to Site 1015.

The primary objective for drilling here was to sample a very high-resolution sediment section for comparison with ODP Site 893 in the Santa Barbara Basin. Hemipelagic sections between turbidites should be sufficiently large to study upper Pleistocene and Holocene paleoceanographic processes. The site should also prove useful for sedimentological study of turbidite deposition and the development of Hueneme Fan. Organic carbon diagenesis will be studied, through detailed pore-water analysis in the upper 100 mbsf geochemical analyses of the solids, in a sedimentary section that has been quickly deposited and that contains

a large terrigenous organic component.

The sedimentary sequence recovered from the two holes at Site 1015 consists of a 150-m-thick interval of upper Quaternary (60 ka) sediments. Sediments consist of one lithologic unit, which is dominated by quartz feldspar sand and clayey silt interbedded at decimeter to meter scale. Sand layers with sharp basal contacts, frequently with wood fragments in the upper part, grading upwards into clayey silt are interpreted as turbidite deposits. Thin layers of laminated hemipelagic nannofossil clay and disseminated volcanic glass occur between the turbiditic sediments. Authigenic pyrite is a minor but common constituent. Calcareous nannofossils and, to a lesser extent, foraminifers dominate the calcareous fraction of the sediments. The biosiliceous component is negligible.

Detailed comparisons between the magnetic susceptibility generated using the MST and high-resolution color reflectance measured using the Oregon State University system at the two holes, demonstrated complete recovery of the sedimentary sequence down to 36 mbsf. The existence of gas voids, turbidites, and coring disturbances below that depth precluded an interhole correlation.

Calcareous nannofossil and planktonic foraminifer data indicate that the 150-m sequence of turbidites and hemipelagic sediments are of latest Quaternary age, younger than 60 ka. Sand layers in the sequence are barren of microfossils except for very rare, moderately well preserved, calcareous nannofossils in some intervals. Hemipelagic sediments contain abundant to few, well-preserved planktonic foraminifers, common to abundant, well-preserved benthic foraminifers, and abundant to rare, well-preserved calcareous nannofossils. Radiolarians and diatoms are essentially absent, except for reworked Miocene taxa.

Changes in planktonic foraminifer assemblages in this sequence exhibit evidence of large-scale Quaternary glacial-interglacial oscillations. The Holocene is well marked by interglacial planktonic foraminifer assemblages. Planktonic and benthic foraminifer assem-

blages suggests that the glacial-interglacial episodes are associated with changes in circulation of upper intermediate waters affecting changes in oxygen levels of the basins of the California Borderland.

Gas voids, turbidites, and coring disturbances precluded the measurement of most physical properties and the determination of a paleomagnetic reversal stratigraphy. Furthermore, the sequence is too young to contain magnetic field reversals.

Carbonate values range from 2 to 7 wt%. Lowest values occur in the turbiditic sequences. The organic carbon record shows hemipelagic background values of about 1 to 1.5 wt%. In the turbidites, organic carbon is below 0.5 wt%. Spikes up to 2.3 wt% result from wood fragments in the sediment. Methane concentrations are high throughout the sediment column, however, no significant amounts of ethane were observed.

Although the chemical composition of the 9 interstitial water samples from this site indicates that organic matter diagenesis, biogenic opal dissolution, and authigenic mineral precipitation and/or ion exchange reactions are significant influences, the nature of the sediments and the effects of drilling and recovery on them make distinguishing primary geochemical signals from contamination of interstitial water samples by seawater drilling fluid problematic.

Site 1016 (Proposed Site CA-11E)

Site 1016 is located about 150 km west of Point Conception, and forms the deep-water site on the Conception Transect (35° N). The site is located on a northeast trending abyssal hill and rises 50–100 m above the surrounding seafloor (Fig. 1) in water 3846 m deep. Basement is 22.5-Ma oceanic basalt. The site was chosen to provide material to investigate the longer term Neogene record as well as to assess paleoceanographic conditions near the

core of the California Current. Site 1016 occupies an important transitional zone for modern flora and fauna, and provides a good opportunity to link magnetochronology and biostratigraphy. Geochemical indices of paleoproductivity and microfossil assemblages obtained from this site will provide important data on nutrients carried by the California Current. Organic carbon deposition should be relatively high compared to typical pelagic sedimentary sections, yet the sedimentation rate is low. This environment provides one of the end members needed to study preservation of bulk organic matter and of specific organic molecules.

The sedimentary sequence recovered from the 4 holes at Site 1016 consists of a well-dated, apparently continuous, 308-m-thick interval ranging from Quaternary to late Miocene age. Sediments are dominated by decimeter to meter scale alternations of carbonate and siliciclastic layers. Several fine-grained sand layers and volcanic ash bands, each up to several centimeters thick, occur in the upper two thirds of the sequence. The base consist of porcellanite and chert horizons of unknown thickness. The sediments are divided into three lithologic units. Unit I (0–71 mbsf) is characterized by the relative abundance of clay and the prevalence of diatom ooze with clay, diatomite, and diatoms with clay. Unit II (71–163 mbsf) contains an increased amount of calcareous nannofossils and is composed of nannofossil ooze with diatoms. This unit is subdivided in two subunits on the basis of carbonate content. Unit III (163–316 mbsf) is dominated by diatomite and diatom ooze, and contains several volcanic ash layers and blebs of solid bitumen. The base of this unit consists of porcellanite and black chert. Sedimentation rates are high, averaging 50 m/m.y. from the Quaternary to the upper Pliocene, are drastically lower during the early to middle Pliocene (10–15 m/m.y.), and average 30 m/m.y. in the late Miocene.

Detailed comparisons between the magnetic susceptibility and GRAPE density record generated using the MST, and high-resolution color reflectance measured using the Oregon State University system, demonstrated complete recovery of the sedimentary sequence down to 245 meters composite depth (mcd), with the exception of a core gap at 172.6 mcd,

which could not be covered by overlap (Fig. 7).

A well-constrained biostratigraphy and chronology is provided by a combination of calcareous nannofossil, planktonic foraminifer, diatom, and radiolarian datums for the upper Pliocene and Quaternary. The upper Miocene to lower Pliocene (below 154 mbsf) is dated by calcareous nannofossils, diatoms, and radiolarians. The base of the sequence is late Miocene (less than 7 Ma) in age. Diatom and radiolarian assemblages suggest two major episodes of strong upwelling during the upper Miocene and the upper Pliocene through lower Quaternary. These two episodes are separated by an interval marked by decreased vertical advection of deep waters during the lower to middle Pliocene, resulting in relatively low sedimentation rate. Cooling at thermocline depths is suggested after 3.0 Ma by Arctic radiolarian assemblages. This was followed at 2.5 Ma by major surface-water cooling. Lower bathyal benthic foraminifer assemblages appear to change little throughout the upper Pliocene and Quaternary, including between glacial and interglacial episodes.

A magnetic polarity stratigraphy could not be obtained because magnetic intensities were below the noise level of the magnetometer.

Calcium carbonate values vary from 1 to 62 wt%. Between about 2 and 6 Ma (75 to 165 mbsf), the $CaCO_3$ values are distinctly higher. Organic carbon concentrations are high compared to normal open ocean environments (average 0.93 wt%). According to organic carbon to total nitrogen ratios, the organic material is mainly of marine origin. Headspace methane values are very low throughout the sediment column, indicating that no significant methanogenesis occurred.

Chemical gradients in the interstitial waters reflect organic matter diagenesis, the dissolution of biogenic opal and calcium carbonate, the diffusive influence of reactions in the underlying basalt, and the influence of authigenic mineral precipitation. Alkalinity increases to peak values >17 mM, phosphate to nearly 60 μM, and ammonium to >2 mM. Calcium

decreases with depth to as low as 5.2 mM, then increases to 13.2 mM. Magnesium decreases throughout the section to 26.1 mM, with the decrease in the lower part of the section linearly correlated to the increase in calcium.

The porosity profiles can be divided into three units corresponding to the three lithological units. The upper 100 mbsf with high porosities around 70%–75% in sediments composed of clays and diatomite, an interval of low porosities oscillating around 60%–70% from 100 to 200 mbsf, in carbonate-rich sediments, followed by an increase of porosity downhole with values between 70% and 80%, in the diatomite-rich unit. Highs in PWL velocity and GRAPE density correspond well with reflections on the 3.5-kHz seismic site-survey record (Fig. 8). The impedance contrasts that generate the reflectors correspond to the sandy turbidite layers in the upper 70 mbsf of the section.

Three good-quality temperature measurements were obtained: 4.9°C at 36.1 mbsf, 7.0°C at 55.1 mbsf, and 9.0°C at 74.1 mbsf. Using an average measured thermal conductivity of 0.838 W/(m·K) provides a heat-flow estimate of 88 mW/m^2.

Major lithologic units were identified using color reflectance data. In Unit I reflectance for the 450–500 nm (blue) band is generally low. As Unit I grades into Unit II, the proportion of nannofossils increases, as does blue band reflectance. Subunit IIB, which is predominantly nannofossil ooze interbedded with diatom ooze, has the highest reflectance of any stratigraphic unit at Site 1016. The signal of Unit IIB is variable: high reflectance values generally match nannofossil-enriched layers, and low values match more diatomaceous zones. In Unit III, diatoms replace nannofossils as the dominant microfossil component, and reflectance is low. The near infrared (nIR; 850–900 nm) to blue (450–500 nm) ratio is generally greatest when the diatom content is greatest and lowest, where clays and nannofossils predominate. These results imply that color reflectance is sensitive to the spectral character of diatom-rich sediments, or a sedimentary component that covaries with the diatom content.

Logging at Hole 1016B consisted of two full passes with the Triple Combination tool string, one full pass with the FMS-sonic tool string, and two full passes with the magnetic susceptibility-total moment tool string. Hole conditions were fair from 220 to 300 mbsf, and excellent above 220 mbsf and up to the base of pipe at about 60 mbsf. The log physical property data closely matched the measured core density, porosity, and magnetic susceptibility over the core-log data overlap. The log variations clearly delineate the major and minor lithologic boundaries, particularly the transition to diatomites. Initial log-core comparisons suggest that decimeter-scale variations in lithology are reliably recorded by the logging tools. This provides the opportunity to assess the degree of rebound and deformation of the core material, and will be especially useful for putting together continuous records even where material is missing at core gaps.

Site 1017 (Proposed Site CA-9D)

Site 1017 is located about 50 km west of Point Arguello on the continental slope just south of Santa Lucia Bank in water 966 m deep (Fig. 1). It is the shallow-water site in the Conception Transect (35°N). The major objective for drilling was to sample a high-resolution, upper Pliocene to Holocene sediment section to compare with Santa Barbara Basin (Site 893). Site 1017 is near an important upwelling center off Point Conception and will be used to define the history and cyclicity of upwelling near 35°N. The oxidation-reduction history at this site will be affected by changes in the oxygen minimum depth through time. Waters drawn into Santa Barbara Basin also come from this vicinity, and data from Site 1017 should confirm whether Santa Barbara Basin oxygenation is being driven by changes in intermediate-water source. The site will also provide important new information about organic carbon diagenesis and about minor-element geochemistry through pore-water profiles and through solid-phase analyses. Pore-water sampling will be used to define the rates of organic matter oxidation and the removal of oxidants from the pore waters and sedi-

ments, whereas organic geochemical analysis will provide data on organic matter preservation in a low-oxygen environment.

The sedimentary sequence recovered from the five holes at Site 1017 consists of a well-dated, apparently continuous, 204-m-thick interval of Quaternary (1.2–1.4 to 0.0 Ma) age. The sediments consist almost entirely of silty clay to clayey silt with minor, variable quantities of intermixed foraminifers, nannofossils, and siliciclastic sand. Thin, discrete layers of quartzofeldspathic or foraminiferal sand turbidites are a frequent, but volumetrically minor, component of the upper two thirds of the sequence. Cemented limestone and dolostone occur at only a few horizons. Bedding is indistinct, gradational, and very thick (about 1 cycle/10 m) until becoming more distinct and thinner (several meter scale) below approximately 125 mbsf. The stratigraphic sequence is grouped into a single lithologic unit, with two subunits. Subunit IA is composed of silty clay to clayey silt. Subunit IB is composed of silty clay to clayey silt, and nannofossil clay mixed sediment, all containing minor amounts of foraminifers and diatoms. Sedimentation rates are around 100–120 m/m.y. on average.

Detailed comparisons between the magnetic susceptibility and GRAPE density records generated using the MST, and high-resolution color reflectance measured using the Oregon State University system, showed that a continuous sedimentary sequence may exist down to about 130 mcd. However, exact tie points between adjacent holes could not be established in most cases and precluded the construction of a spliced section.

Calcareous nannofossils are of highly variable abundance and quality of preservation throughout the sequence. The section above 175 mbsf is marked by mostly abundant to common and well-preserved planktonic and benthic foraminifers. Below 175 mbsf to the base of the hole, the section is essentially barren of planktonic foraminifers and benthic foraminifers are either absent or occur in low abundances. Diatoms are almost exclusively limited to reworked forms and radiolarians are absent to rare in the sequence. Changes in

planktonic foraminifers indicate strong glacial to interglacial oscillations throughout. Overall, both interglacial and glacial planktonic foraminifer assemblages reflect relatively cooler conditions than in all earlier drilled sequences of Leg 167. This is almost certainly because of the sites location in the heart of the coastal upwelling zone off Point Conception.

Benthic foraminifer assemblages exhibit large differences between glacial and interglacial episodes. Assemblages associated with glacial episodes reflect relatively higher oxygen concentrations of bottom waters, whereas those associated with interglacial episodes reflect distinctly lower oxygen concentrations in bottom waters, as in Santa Barbara and Tanner Basins.

Other materials observed in the sand-sized fraction of many of the core-catcher samples include prominent fish debris, including fish scales, charcoal fragments, sponge spicules, and echinoid spines. Also observed were large numbers of tar (asphalt) globules that have glued together a variety of biogenic materials, especially sponges spicules. The tar was almost certainly derived from natural oil seeps in the region during the entire Quaternary.

After AF demagnetization, the magnetization of most cores was just around the sensitivity limit of the magnetometer. With the exception of one single section, there was no interval of reverse polarity in Hole 1017B. The positive inclinations of the top 110 mbsf represent most likely the Brunhes Chron C1n. Below the normal polarity interval, an interpretation of the inclination record was not possible because of the low magnetic intensity and core disturbance by XCB coring.

Sediments at Site 1017 are characterized by carbonate values ranging from 2 to 12 wt%. At 130 mbsf, an increase in the concentration and fluctuation can be observed. The organic carbon concentration shows a similar increase with depth from average values of about 1.5 to 2.7 wt% at 170 mbsf. The C to N ratio record displays a remarkably low fluctuation

around the average value of 10. A good correlation between $U^{k'}_{37}$, C_{37} alkenone abundance, and total organic carbon content (Fig. 9) exists. Both C_{37} alkenone abundance and total organic carbon content show higher concentrations in warmer (interglacial) than in cooler (glacial) periods.

Volatile hydrocarbons are high throughout the sediment column, but no significant amounts of ethane could be detected, indicating that no thermogenic hydrocarbons occurs.

Chemical gradients in the interstitial waters (Fig. 4) reflect organic matter diagenesis, the dissolution of biogenic opal and calcium carbonate, and the influence of authigenic mineral precipitation reactions. Alkalinity increases to peak values >40 mM, whereas sulfate concentrations decrease to values below the detection limit (approximately 1.4 mM) by 19.25 mbsf. Phosphate concentrations increase to values >100 µM and ammonium concentrations increase to an average of 8.5 mM. Dissolved silicate increases to concentrations near 1000 µM, and strontium increases to >150 µM. Calcium concentrations decrease to around 2.4 mM, then increase with increasing depth to 5.3 mM. Magnesium concentrations generally decrease throughout the section.

Velocities shallower than 10 mbsf were high, ranging from 1586 to 1607 m/s. Below this depth, gas expansion attenuated the signal and precluded the determination of further velocity measurements. Downhole temperature measurements gave a thermal gradient of 74°C/km (Fig. 5). Using an average thermal conductivity of 0.937 W/(m·K) yields a heat-flow estimate of 70 mW/m^2 at Site 1017.

Site 1018 (Proposed Site CA-8A)

Site 1018 is located about 75 km west of Santa Cruz, California, on a sediment drift just south of Guide Seamount at a water depth of 2477 mbsl (Fig. 1). The primary objectives at this site were to sample a high-resolution upper Miocene to Holocene sediment section from the central California Margin to study evolution of the California Current, as well as the history of upwelling and productivity. It provides continuity between the Gorda Transect at 40° N and the southern California Transects. The site also provides a dipstick to sample midwaters during the time in which the Northern Hemisphere ice sheets were formed. It will also be used to collect new data on organic carbon diagenesis and minor-element geochemistry through pore-water profiles and solid-phase analyses. Organic carbon contents and terrestrial organic matter input should be moderately high. Pore-water sampling will be used to define the rates of organic matter oxidation and the removal of oxidants from the pore waters and sediments, whereas organic geochemical analysis will provide data on organic matter preservation underneath a well-oxygenated water column.

The sedimentary sequence recovered from the 4 holes at Site 1018 consists of a well-dated, apparently continuous, 426-m-thick interval of uppermost lower Pliocene to Quaternary (3.5–0.0 Ma) sediments. Sediments vary from siliciclastic to interbedded mixtures of biogenic and siliciclastic components. Siliciclastic clays are found throughout the cored interval, but are predominant in the upper part. The middle part is dominated by diatom clay and diatom clay mixed sediment with frequent interbedding of clayey nannofossil ooze, whereas the lower part is dominated by interbeds of nannofossil clay and clayey nannofossil chalk. Diatomaceous layers tend to correspond to darker and less bioturbated intervals compared to nannofossil-rich layers. Fine-grained feldspar quartz sand occurs as thin normally graded layers (possibly turbidites), especially in the upper part of the sequence, whereas glauconite occurs both as discrete layers and disseminated in the clay matrix in the lower part of the sequence. Vitric volcanic ash layers are rare except in the lowermost part of the sequence.

The sediments are divided into two lithologic units. Unit I is a siliciclastic unit composed mainly of clays with varying amounts of diatoms and sporadical occurrence of nannofossils. Unit II is characterized by continuous and slightly increasing content of nannofossils and slightly decreasing content of diatoms.

Detailed comparisons between the magnetic susceptibility and the GRAPE density record generated using the MST, and high-resolution color reflectance measured using the Oregon State University system, demonstrated complete recovery of the sedimentary sequence down to 193 mcd. Sedimentation rates range from 100 to 200 m/m.y. and average 130 m/m.y.

A well-constrained biostratigraphy and chronology is provided by a combination of calcareous nannofossil, planktonic foraminifer, radiolarian, and diatom datums for the upper Pliocene and Quaternary. Planktonic foraminifers suggest that the base of the section is about 3.4 Ma in age. All microfossil groups are clearly dominated by cool, high-latitude elements throughout the late Neogene. Site 1018 is sufficiently far north in the California Current to exclude most to all subtropical elements even during interglacial episodes. Radiolarians are entirely represented by subarctic forms. Diatoms are dominated by subarctic forms with the addition of much less abundant temperate elements. Planktonic foraminifer assemblages are dominated by subarctic to cool temperate forms, and subtropical elements are absent, except during warmest interglacial episodes. Planktonic foraminifers exhibit glacial to interglacial oscillations throughout. Radiolarians, however, do not exhibit such changes, almost certainly because they largely live at greater water depths.

Changes in microfossil assemblages provide evidence of progressive cooling during the late Neogene. The first consistent occurrence of mostly common to abundant populations of sinistrally coiled *Neogloboquadrina pachyderma* marks a distinct cooling step at about 1.3 Ma. Likewise, changes in radiolarian assemblages indicate a further step towards cool-

er conditions at about 1.0 Ma. Diatoms are dominated by oceanic forms, but during the Quaternary include a small but distinct littoral assemblage that typically lives on sea grass. These forms were reworked from shallow waters, and appear to be most abundant during times of higher input of terrigenous sediments.

Positive paleomagnetic inclinations of the top 88 mbsf most likely represent the Brunhes Chron C1n. Below the normal polarity interval, an interpretation of the inclination record was not possible because of the low magnetic intensity and core disturbance by XCB coring.

Calcium carbonate contents are very low, ranging from 0 to 5 wt% in the upper 350 mbsf. Spikes of high values up to 17 wt% frequently occur. In the lower part of the column, $CaCO_3$ concentrations distinctly increase to values between 5 and 25 wt%. Total organic carbon variation is very stable around an average value of 1.2 wt%. The organic material is mainly of marine origin, as indicated by low C to N ratios of about 6 to 8. This is also supported by very high methane concentrations throughout the sediment column. No significant amounts of ethane or propane were observed in the headspace samples.

Chemical gradients in the interstitial waters (Fig. 4) reflect organic matter diagenesis, the dissolution of biogenic opal and calcium carbonate, the influence of authigenic mineral precipitation reactions, and the diffusive influence of reactions in underlying basalt. Alkalinity increases to peak values >50 mM, whereas sulfate concentrations decrease to values below the detection limit (approximately 1.3 mM) by 9.35 mbsf. Phosphate concentrations increase to values >160 μM, and ammonium concentrations increase to maximum values >7 mM. Dissolved silicate increases to concentrations >1000 μM, and strontium increases to >250 μM. Calcium concentrations decrease to as low as 3.6 mM, then increase with increasing depth to 11.5 mM. Magnesium concentrations generally decrease throughout the section to values as low as 22 mM.

The porosity decreases downhole to 70 mbsf, scatters around a constant value until about 345 mbsf, and then continues to decrease downhole. This trend corresponds well with the lithological boundaries. The diatom-rich unit between 200 and 345 mbsf represents an interval of low grain densities. The increase of bulk and grain densities and decrease of porosity at 345 mbsf correspond to the increase in carbonate concentration in the nannofossil-rich unit. High-resolution opal content was predicted using a multiple linear regression equation generated from site-survey color reflectance and opal data (Fig. 10). Results are consistent with the major lithologic units, and indicate an average opal content of 1.96 wt%.

In situ temperature measurements at Site 1018 gave a thermal gradient of 32°C/km (Fig. 5). Using an average measured thermal conductivity of 0.847 W/(m·K) yields a heat-flow estimate of 27 mW/m^2.

Logging conditions at Hole 1018A were poor. A ledge at approximately 220 mbsf was encountered, and one pass with the Triple Combination tool string was made from 220 mbsf to the mudline. Pipe was then set at 240 mbsf and a second pass with the Triple Combination tool string was made from 350 mbsf, where another ledge was found, up to the base of pipe at 240 mbsf. Because of poor hole conditions with many washouts, and difficulties with lowering the tool string past ledges in the borehole, logging with the FMS and Geological High-Sensitivity Magnetic Tool (GHMT) string was not attempted.

Site 1019 (Proposed Site CA-1D)

Site 1019 is located about 60 km west of Crescent City, California, in the Eel River Basin at a water depth of 983 mbsl (Fig. 1). It is the nearshore site of the Gorda Transect. The primary drilling objective was to sample a high-resolution Pleistocene sediment section as part of the coastal transect from 30° to 40° N and as part of the Gorda Transect across the California Current at 40° N. Site 1019 should will provide important information about the

development of coastal upwelling as glaciation expanded in the Northern Hemisphere. It will provide important new information about organic carbon diagenesis and about minor-element geochemistry through pore-water profiles and through solid-phase analyses. One of the important objectives at this site was to study the formation of the bottom-simulating reflector (BSR) and to sample gas hydrates. A high-resolution pore-water sampling program was carried out to detect evidence of gas hydrate formation. A logging program was added to measure the extent of gas hydrate formation in situ.

A 247-m-thick sequence of upper Quaternary (1.0–0.0 Ma) sediment was recovered at Site 1019. The sediments consist of one single lithological unit that is subdivided into two subunits. Subunit IA (0–30 mbsf) is a mixed siliciclastic and biogenic unit composed mainly of clays and silt with varying amounts of diatoms and nannofossils. Abundant laminae and thin sand beds occur throughout the middle to lower parts of this subunit. Subunit IB (30–246.4 mbsf) is composed predominantly of siliciclastic clays and silts with a minor diatom component and absent or rare nannofossils. Laminae and thin sand beds occur only in the middle part of this subunit. Sedimentation rates are extremely high (400–1000 m/m.y.) until about 800 ka. After this, rates of sedimentation drastically decreased (to about 150 m/m.y.), and further decreased to about 100 m/m.y. following 450 ka. The decreased rate of sedimentation after 800 ka probably resulted from the tectonic development of the bank immediately to the east of Site 1019. Once this bank was of sufficient elevation, it would have blocked the sediment transport from the adjacent continental shelf. Conspicuous glauconite also began to be deposited at 800 ka at the time of reduction in sedimentation rates, and probably reflects its formation on the developing bank. If this is correct, 250 m of bank uplift occurred in 800 k.y., which is 3 cm/100 yr; a very rapid rate of uplift rate associated with the well-known regional neotectonism.

Detailed comparisons between the magnetic susceptibility and the GRAPE density record generated using the MST, and high-resolution color reflectance measured using the Oregon State University system, demonstrated complete recovery of the sedimentary sequence down to 86 mcd.

Biostratigraphy provides limited age control for the sequence at this site. The base of Hole 1019C is dated at about 1 Ma. The middle part of the sequence is dated using the onset of the prominent 100-k.y. paleoclimatic oscillations at 800 ka (at 113 mbsf) and the upper part by a combination of calcareous nannofossil, radiolarian, and diatom datums. Planktonic foraminifer assemblages reflect oscillations between glacial and interglacial episodes. These faunas are marked by cooler elements during both glacial and interglacial episodes, compared to previous Leg 167 sites to the south (Sites 1010 to 1018). Radiolarians are completely dominated by subarctic forms, whereas diatoms are dominated by cool, high-latitude, North Pacific assemblages, with limited subtropical forms. Radiolarian and diatom taxa characteristic of upwelling are inconspicuous at this site, and diatom assemblages contain rare but pervasive coastal planktonic forms. Benthic foraminifer assemblages indicate the presence of relatively low oxygen concentrations in bottom waters throughout the entire sequence. Intervals marked by particularly low oxygen levels occur in the uppermost part of the sequence, younger than 250 ka (above 27.3 mbsf).

Positive paleomagnetic inclinations of the top 75 mbsf most likely represent the Brunhes Chron C1n. Below the normal polarity interval an interpretation of the inclination record was not possible because of core disturbance by XCB coring.

The methane concentration increased in the second core to maximum values and caused frequent gas voids in the recovered cores. Although the gas pressure was very high, no significant amounts of higher hydrocarbons were found. Calcium carbonate concentrations are generally low, and show a fluctuation between 0 and 9 wt%. Total organic carbon varies from 0.5 to 1.5 wt% throughout the sediment section. According to the C to N ratios, the organic fraction is mainly consisting of marine-derived material.

The most striking feature of the chemical gradients in the interstitial waters (Fig. 4), sampled at 1 per core throughout the site, is a pronounced decrease in chlorinity, from 551 mM

at 4.45 mbsf to an average of 357 mM at >150 mbsf. The smooth shape of the profile and the lack of dilution in other elemental concentrations are not consistent with the low chlorinity resulting from an artifact of methane hydrate dissociation, instead indicating there must be a source of low-chlorinity fluid in contact with the site. Other chemical gradients reflect organic matter diagenesis, the dissolution of biogenic opal, the influence of ion exchange and authigenic mineral precipitation reactions, and the diffusive influence of reactions in underlying basalt. Alkalinity increases to peak values >95 mM, whereas sulfate concentrations decrease to values below the detection limit (ca. 0.5 mM) by 12.75 mbsf. Phosphate concentrations increase to strikingly high values >340 µM, and dissolved silicate increases to concentrations >1000 µM. Calcium concentrations decrease to a minimum <1 mM at 41 mbsf, then increase with increasing depth to 4.0 mM at 242 mbsf. Magnesium concentrations decrease to a minimum of 25 mM, coincident with the Ca minimum, then increase with increasing depth to 37–39 mM, subsequently decreasing to 31.5 mM at 242 mbsf. There are no apparent changes in the interstitial water profiles at the estimated depth of the BSR.

The 4 Adara temperature measurements yield a thermal gradient of 57°C/km (Fig. 5). Using an average measured thermal conductivity of 0.989 W/(m·K) provides a heat-flow estimate of 57 mW/m^2. The index properties data show a sharp decrease in bulk density values down to about 30 mbsf, which coincides with the lithostratigraphic Subunit IA and IB boundary. Below this, index properties values are fairly constant, with occasional fluctuations generally corresponding to lithologic variations.

Color reflectance was generally low, averaging 10% in the visible wavelengths. Downhole variability in the reflectance signal was minimal (standard deviation of 1%). A prediction of opal content was made using a multiple linear regression equation derived from site-survey reflectance and opal measurements. The results were consistent with the lithologic subunits described at Site 1019, showing higher opal content in Subunit IA than in Subunit IB.

Hole 1019C was logged with one full pass of the Triple Combination tool string, two FMS-Sonic passes, and two GHMT passes. Caliper measurements indicated that the borehole was in poor condition, with broad, irregular washouts throughout the logged interval. The hole was highly elliptical in shape with the long axis oriented north-south, consistent with borehole breakout resulting from the regional east-west maximum compressive stress orientation. The poor hole conditions adversely affected those measurements requiring good contact with the borehole wall (e.g., density, porosity, and FMS), although comparision with core-based physical property data demonstrated that the log measurements were valid over most of the hole where good contact was established. The log data were intended to determine the origin of the BSR observed in the seismic profiles of this site. The log data did not indicate any corresponding increases in sonic velocity or density reductions that typically characterize clathrate occurrances. There was, however, an anomalously high-resistivity layer at ca. 100 mbsf (about 5 m thick) that was not associated with corresponding density or velocity increases.

Site 1020 (Proposed Site CA-4A)

Site 1020 is located on the east flank of the Gorda Ridge at a water depth of 3040 mbsl (Fig. 1). It is about 170 km west of Eureka, California, and forms the high-resolution, deep-water site on the Gorda Transect. The site is located on an abyssal hill which trends northeast and rises 50–100 m above the surrounding seafloor on 5.1-Ma ocean crust. The primary objective of drilling at this site was to study paleoceanographic conditions near the core of the Northern California Current during the critical time interval when the Northern Hemisphere ice sheets began to form. The development of a correlation between biostratigraphy and the paleomagnetic chronostratigraphy was another key objective at this site. Site 1020 will provide information about organic carbon diagenesis and about minor-element geochemistry through pore-water profiles and through solid-phase analyses. Paleomagnet-

ic studies will provide an avenue to study the deformation of the Gorda Plate. Provided that stable magnetic declinations can be obtained, the rotation of the Gorda Plate can be monitored through time. A secondary goal was to obtain a representative sample of the basalt basement for igneous petrology and geochemistry.

The sedimentary sequence recovered from the 4 holes at Site 1020 consists of a well-dated, apparently continuous, 275-m-thick interval of upper lower Pliocene to Quaternary (3.79–0.0 Ma) sediments. Siliciclastic clay is found throughout the cored interval and is the dominant component in the upper part of the sequence. The middle part is dominated by nannofossil clay with frequent interbedding of clayey nannofossil ooze. Diatoms are also present, but only as a minor component ranging from 10% to 30% of the total sediment. The lower portion is dominated by interbeds of nannofossil clay and clayey nannofossil chalk. Two thin (decimeter-scale) intervals of dolomite are found at 78 mbsf and 178 mbsf. Turbidite deposition is relatively unimportant at this site compared to previous sites except for a few thin, graded beds in the uppermost portion and a slightly thicker interval at about 68 mbsf. Lithostratigraphic Unit I is predominantly composed of clay-rich sediments mixed with minor quantities of nannofossils and diatoms. Thin intervals of nannofossil ooze occur throughout this unit, and diatoms rarely exceed 30% of the sediment. Unit II consists of clayey nannofossil chalk mixed sediments in which pyrite nodules are abundant and scattered throughout. Clay content increases to nearly 95% near the bottom. Approximately 5 cm of basalt was recovered at the base of the hole.

Detailed comparisons between the magnetic susceptibility and the GRAPE density record generated using the MST, and high-resolution color reflectance measured using the Oregon State University system, demonstrated complete recovery of the sedimentary sequence down to 242 mcd, with the exception of coring gaps at 126, 137, and 200 mcd, which could not be covered by overlap. Bulk densities in the upper part of the section slowly increase downhole with some scatter corresponding to the interbedding of clay and nannofossil clay. Densities are constant between 120 and 220 mbsf and increase sharply at 220 mbsf.

The increase is caused by higher carbonate content, corresponding to the top of the nannofossil chalk mixed with clay.

A well-constrained biostratigraphy and chronology is provided by a combination of calcareous nannofossil, planktonic foraminifer, radiolarian, and diatom datums, and paleomagnetic reversals for the upper lower Pliocene and Quaternary. Most of the sequence contains common radiolarians and mostly common to abundant diatoms. All of the microfossil groups are clearly dominated by cool, high-latitude elements throughout the late Neogene. Radiolarians are entirely represented by subarctic forms, and the assemblages exhibit noticeably lower diversity than at all other sites cored during Leg 167. Diatoms are dominated by North Pacific subarctic assemblages in addition to rare temperate elements. Relative high abundances of *Gephyrocapsa carribeanica* may indicate cooler episodes within the Quaternary. Planktonic foraminifer assemblages are dominated by subarctic to cool temperate forms, with subtropical elements absent. Radiolarians are represented by forms not characteristic of upwelling regions throughout the entire sequence. Likewise, diatoms are represented by open-ocean forms not characteristic of coastal upwelling regions, except during the early late Pliocene when upwelling forms are present in relatively low frequencies.

Planktonic foraminifer assemblages are made up entirely of cool temperate to subarctic taxa. Distinct changes in planktonic foraminifer assemblages in the uppermost Pliocene and Quaternary clearly reflect glacial to interglacial oscillations. In contrast, radiolarians do not. At greater depths in the section, short-term, climatically related faunal changes are much less conspicuous. Late early Pliocene planktonic foraminifers (3.8 Ma) exhibit the highest diversity in the sequence, and are considered to reflect the warmest surface-water temperatures. The first consistent occurrence of sinistrally coiled *Neogloboquadrina pachyderma* marks a distinct cooling step at 1.14 Ma.

Benthic foraminifers in the upper Pliocene and Quaternary are typical lower bathyal, deep-

sea assemblages indicative of well-oxygenated bottom waters. The faunas exhibit little change throughout the entire upper Pliocene and Quaternary, and exhibit no clear oscillations associated with glacial/interglacial change. In the lowermost part of the section, the benthic foraminifer assemblages may represent deposition in lower middle bathyal water depths as compared with lower bathyal depths in the sequence above. The changes in benthic foraminifer assemblages represent evidence for rapid tectonic subsidence in the lower 30 m of the sequence. The changes in benthic foraminifers would indicate subsidence of 500 to 1000 m during this interval. No evidence for paleodepth change is evident from benthic foraminifers above 256 mbsf during the late early Pliocene through Quaternary.

AF demagnetization at 20 mT revealed a complete magnetostratigraphic record between 0 and 130 mbsf that allowed the identification of the Brunhes (C1n) and the Jaramillo (C1r.1n) normal polarity intervals. Reorientation of the magnetic declination using the Tensor tool supports the interpretation of magnetic polarity zonation based on the inclination data.

Headspace volatile hydrocarbon concentrations range from 5 to 8900 ppm methane. Ethane or propane gases are near the detection limit. Low calcium carbonate concentrations between 1 and 20 wt% were found in the upper 220 mbsf. Below this depth, $CaCO_3$ concentrations increase up to 58 wt%. Organic carbon contents vary around 0.7 wt%, and show slightly decreased values where carbonate content is high. Low total organic carbon to total nitrogen ratios between 4 and 9 indicate a marine dominance of the organic material.

Chemical gradients in the interstitial waters reflect organic matter diagenesis, the dissolution of biogenic opal and calcium carbonate, the influence of authigenic mineral precipitation reactions, and the diffusive influence of reactions in underlying basalt. Alkalinity increases to peak values of >20 mM, whereas sulfate concentrations decrease to values be-

low the detection limit (approximately 0.2 mM) by 107.25 mbsf. Phosphate concentrations increase to values >55 μM, and ammonium concentrations increase to maximum values >3 mM. Dissolved silicate increases to concentrations >1000 μM, and strontium increases to 230 μM. Calcium concentrations decrease to as low as 5.2 mM, then increase with increasing depth to 26.3 mM at 260.30 mbsf. Magnesium concentrations generally decrease throughout the section to 19.6 mM at 260.30 mbsf.

The 4 Adara temperature measurements yield a thermal gradient of 189°C/km. Using an average measured thermal conductivity of 0.899 W/(m·K) provides a heat-flow estimate of 170 mW/m^2 at Site 1020 (Fig. 5). The vicinity of the Gorda Ridge explains this relatively high heat-flow value.

Reflectance data are consistent with the major lithological units. In lithostratigraphic Unit I reflectance is consistently low for the 450–500 nm band. Unit II shows greater and more variable reflectance than Unit I. A ratio of the 850- to 900-nm (nIR) band to the 450- to 500-nm (blue) band was used as a qualitative proxy for opal content. In Subunit IA, where clay predominates, the nIR/blue is generally low. As Subunit IA grades into Subunit IB, the proportion of diatoms increases, as does the mean value and variability of the ratio of nIR to blue.

Hole 1020B was logged with the Triple Combination, FMS/Sonic, and GHMT tool strings from 86 to 275 mbsf. Overall log quality at this site was excellent to very good below 170 mbsf, and fair in the washed out section above 170 mbsf. Comparison between the log and core MST data demonstrate that the logs can reliably reproduce first-order features of the records generated from measurements of the sediments using the MST track particularly in the interval below 170 mbsf where hole conditions are very good. Core-log comparison suggests that the cored sediment, and therefore the mcd scale, is expanded by about 10% relative to its true depth range.

Site 1021 (Proposed Site CA-5A)

Site 1021 is the deep-water site of the Gorda Transect (Fig. 1). It is located about 100 km south of the Mendocino Fracture Zone, more than 360 km from the California Coast, and is situated on an abyssal hill at 4240 mbsl on 29.6-Ma crust. The primary drilling objective was to sample the longer term Neogene record, and to develop a correlation between Neogene biostratigraphic data from the northeastern Pacific and the paleomagnetic chronostratigraphy. Because subtropic and subarctic flora and fauna mix along the coast of California, the detailed biostratigraphy fits imperfectly with schema developed for either the tropics or the subarctic North Pacific. Site 1021 will also be used to study preservation of bulk organic matter and, if reliable paleoproductivity indices can be generated, to relate organic matter preservation to flux in low sedimentation rate environments.

The sedimentary sequence recovered from the 4 holes at Site 1021 consists of a well-dated, apparently continuous, 310-m-thick interval of uppermost middle Miocene to Quaternary (11.8–0 Ma) sediments. Sediments are dominated either by homogenous clay-rich intervals or by submeter-scale alternation of carbonate/biosiliceous and siliciclastic strata. All sediments contain biogenic assemblages, mainly calcareous nannofossils, diatoms, foraminifers, and radiolarians, in general order of decreasing abundance. Dominant lithologies are clay, clay with nannofossils/nannofossil ooze, and clayey diatomite/diatom clay mixed sediment. The upper part of the sequence is characterized by a dominance of calcareous nannofossils, whereas diatoms form the main biogenic component in the lower part. Fine-grained volcanic ash layers, and thin clay-rich laminations interpreted as altered ash, serve as potential marker horizons throughout the sequence. The sediments are slightly to moderately bioturbated, with increasing intensity downhole. The sedimentary succession consists of two distinct units (Units I and II) as determined by visual core descriptions and smear-slide estimates. Subunits IA, IB, IC, and IIA and IIB are distinguished by different levels of clay, carbonate, and biogenic silica. Sedimentation rates for the last 10 m.y. were remarkably constant at 30 m/m.y., and decreased during the late middle Miocene (10 to

11.8 Ma).

Index properties correspond well with lithological variations. High grain densities are typical in the nannofossil-rich interval in the upper 110 mbsf and, lower grain densities and higher porosities in siliceous, diatom-rich parts of the sequence (110–310 mbsf).

Detailed comparisons between the magnetic susceptibility and the GRAPE density record generated using the MST, and high-resolution color reflectance measured using the Oregon State University system, demonstrated complete recovery of the sedimentary sequence down to 185 mcd.

A well-constrained biostratigraphy and chronology is provided by a combination of calcareous nannofossil, planktonic foraminifer, radiolarian, and diatom datums, and paleomagnetic reversals. Radiolarians indicate that the base of Hole 1021B is 11.8 Ma in age.

The microfossil groups at Site 1021 are clearly dominated by cool, high-latitude elements from the latest Miocene through the Quaternary. Planktonic foraminifer assemblages are especially cool during Quaternary glacial episodes and the latest Miocene. Radiolarian assemblages suggest relatively warmer conditions during the middle and early late Miocene. Radiolarian species characteristic of upwelling environments are scarce throughout most of the sequence, suggesting weak and episodic vertical advection of deep waters at this location. However, both radiolarians and diatoms indicate that upwelling was stronger during the middle through late Miocene and especially strong during the latest Miocene. Benthic foraminifers indicate that well-oxygenated bottom waters bathed Site 1021 throughout the entire late Neogene.

A complete magnetostratigraphy was determined at Holes 1021B and 1021C after AF demagnetization at 20 mT (Fig. 11). All chrons from the Brunhes (C1n) to the onset of C3n.4n (Thvera subchron) at 5.23 Ma could be identified in the upper 160 mbsf. This sec-

tion will serve as a well-dated reference for the calibration of biostratigraphic datums.

Organic carbon contents are very low, varying between 0.05 and 0.6 wt%. Concentrations are decreasing downhole to values that are typical for pelagic sediments. The total nitrogen contents varies between 0.06 and 0.17 wt%, and the total sulfur content ranges from 0 to about 0.3 wt%. The low C/N ratios indicate a predominant marine origin of the organic material. Two intervals (86–105 mbsf and 222–275 mbsf) show high $CaCO_3$ concentrations of up to 60 wt%. Low $CaCO_3$ concentrations are observed in intervals (0–86 mbsf and 105–275 mbsf) of carbonate dissolution.

Chemical gradients in the interstitial waters reflect organic matter diagenesis, the dissolution of biogenic opal, and possibly the diffusive influence of reactions in underlying basalt. Alkalinity increases to peak values of >9 mM, whereas sulfate concentrations decrease to plateau values around 20 mM by 107.45 mbsf. Phosphate concentrations are greater than 15 μm from 2.96 to 78.95 mbsf, and ammonia concentrations increase to maximum values >500 μM. Dissolved silicate increases to concentrations >1000μM. Calcium concentrations decrease to 8.7 mM at 107.45 mbsf, then increase with increasing depth to 12.5 mM at 304.95 mbsf. Magnesium concentrations gradually decrease throughout the section to 47 mM at 304.95 mbsf.

Downhole temperature measurements yield a thermal gradient of 54°C/km (Fig. 5). Using an average measured thermal conductivity of 0.849 W/(m·K) provides a heat-flow estimate of 46 mW/m^2.

Site 1022 (Proposed Site CA-2B)

Site 1022 is situated on the continental slope just south of the Mendocino Fracture Zone about 90 km from Cape Mendocino. The site is located at a depth of 1950 mbsl on a sliver of continental crust apparently carried seaward along the Mendocino Fracture Zone (Fig.

1). The main objective for drilling at Site 1022 was to obtain a record of surface- and deep-water properties from the Miocene through the Quaternary. Because this site is located only 90 km from the coast, the sediments should provide a good record of coastal upwelling. Site 1022 has important geochemical objectives. Organic carbon deposition should be relatively high, yet the geothermal gradient should be relatively low. This environment provides one of the end members needed to study preservation of bulk organic matter and of specific organic molecules. Geochemical indices of paleoproductivity and microfossil assemblages obtained from Site 1022 will also provide important data on nutrients carried by the California Current and upon how the carbon cycle can be affected by changes in productivity and climate.

The sedimentary sequence recovered from the three holes at Site 1022 consists of a 388-m-thick interval of Quaternary to early Pliocene (0.0–5.0 Ma) age. The sequence is divided into three parts: an upper nannofossil-dominated interval, a middle siliciclastic-clay-dominated interval, and a lower biosiliceous interval. These lithostratigraphic units are further divided into subunits based on minor changes in composition or diagenesis. The uppermost part of the sequence is marked by a 1- to 3-m-thick bed of glauconitic clay with silt and diatoms that represents the entire Quaternary. Below this layer, the upper part of the sequence is dominated by nannofossil clay to nannofossil ooze and diatom clay. This unit includes minor volcanic ash and barite-cemented horizons. The middle part of the sequence is dominated by clay to diatom clay with infrequent interbeds of clayey nannofossil ooze. Diatom content gradually increases from the middle part to the lower unit which is dominated by diatomite and clayey diatomite. A diagenetic boundary occurs at 360 mbsf where diatomite is transformed into interbedded siliceous mudstone and chert. Infrequent, decimeter-thick, dolostone beds occur in all parts of the sequence.

Detailed comparisons between the magnetic susceptibility and the GRAPE density record generated using the MST, and high-resolution color reflectance measured using the Oregon State University system, demonstrated complete recovery of the sedimentary sequence

down to 170 mcd. The bulk densities decrease downhole with some scatter caused by varying clay content. This corresponds to the transition of sediments from nannofossil rich in the upper part to more diatom rich in the bottom of the section. Clay-rich intervals are indicated by high natural gamma radiation activity.

Hole 1022A consists of 166 m of upper Pliocene through possible uppermost lower Pliocene sediments. The Quaternary is represented only by a very thin (<1 m) veneer of sediments overlying the upper Pliocene. The total age range of the sedimentary sequence recovered from Holes 1022A and 1022B is not well constrained. Planktonic foraminifers indicate that the top of the sequence is >2.25 Ma and that the base of Hole 1022A is older than 3.3 Ma. Calcareous nannofossils indicate that the age of the base of Hole 1022A is <3.8 Ma. Because the sequence is relatively thick, each of the 4 groups examined are represented by only one or two biozones and few datums are recognized.

All of the microfossil groups in Holes 1022A and 1022B are represented by cool, relatively high-latitude assemblages. Radiolarians are entirely represented by subarctic forms. Diatoms are dominated by North Pacific subarctic assemblages. Planktonic foraminifer assemblages are dominated by subarctic to cool temperate forms, with subtropical elements absent. Both diatoms and radiolarians show evidence of strong upwelling throughout the Pliocene. The sequence at Site 1022 is the most diatomaceous of late Pliocene age of all Leg 167 sites. Radiolarians indicate a prevalence of strong coastal upwelling; whereas the diatoms reflect oscillations between strong coastal upwelling and oceanic upwelling. Benthic foraminifers throughout are typical middle bathyal, deep-sea assemblages indicative of well-oxygenated bottom waters.

Low magnetic intensities and a drilling-induced overprint precluded the establishment of a magnetic chronostratigraphy.

Volatile hydrocarbon concentrations were very high. Gases up to C6 occurred at about 100

mbsf in the sediment, probably derived from thermogenic degradation of organic material. Although methane/ethane ratios are decreasing with depth, no indication of migrated hydrocarbons was observed. Calcium carbonate values increased within the upper 100 mbsf to a maximum of about 30 wt%, and decreased again to minimum values of 5 wt% at the bottom of Hole 1022A. Organic carbon concentrations varied between 0.5 and 1.5 wt%, showing slightly increased values in lithological Unit II. According to the C to N ratios, organic matter is mainly of marine origin.

Chemical gradients in the interstitial waters reflect organic matter diagenesis, the dissolution of biogenic opal and calcium carbonate, the influence of authigenic mineral precipitation reactions, and the diffusive influence of reactions in underlying basalt. Alkalinity increases to >15 mM, whereas sulfate concentrations decrease to values below the detection limit (approximately 0.4 mM) by 37.45 mbsf. Phosphate concentrations increase to values >65 μM increase to 5.7 mM. Dissolved silicate increases to concentrations >1000 μM, and strontium increases to 182 μM. Calcium concentrations decrease to as low as 4.1 mM, then increase with increasing depth to 6.4 mM at 160.95 mbsf. Magnesium concentrations generally decrease throughout the section to 23.4 mM at 160.95 mbsf.

The 4 Adara downhole temperature measurements yield a thermal gradient of 88°C/km (Fig. 5). Using an average measured thermal conductivity of 0.950 W/(m·K) provides a heat-flow estimate of 84 mW/m^2 at Site 1022.

CONCLUSIONS

Leg 167 drilled 13 sites along the climatically sensitive California Margin: Sites 1010–1022. These sites are arrayed in a series of depth and latitudinal transects to reconstruct the Neogene history of deep, intermediate, and surface ocean circulation, and to understand the paleoclimatic and geochemical history of this region. Leg 167 sites provide an opportunity to address paleoceanographic questions about the evolution of the California Current and

the links between high and low latitudes from millennial and orbital to tectonic time scales. Shipboard results document the suitability of these sediments for addressing these questions. Sites have continuous records of sedimentation at high sedimentation rates, with calcium carbonate present throughout the records, and foraminifers for oxygen- and carbon-isotopic studies are generally abundant. Pioneering biostratigraphy will refine the chronostratigraphic control for this otherwise poorly constrained oceanic regime. Magnetostratigraphy constrains the age models at many sites, and advances in understanding magnetic reversals and the effects of sediment diagenesis on magnetic signals will be possible from these sediments. Significant variations occur in sediment properties on all time scales, as seen in high-resolution nondestructive shipboard measurements (e.g., bulk density, magnetic susceptibility, natural gamma-ray activity, all from the multisensor track, and color reflectance and color video imaging), high- to intermediate-resolution downhole log measurements (e.g., bulk density, resistivity, and magnetic susceptibility), and lower-resolution discrete shipboard measurements (e.g., physical properties and carbon geochemistry). Key topics for investigation include variations in productivity, upwelling, sea-surface temperature, hydrography, sedimentation fluxes, and carbon and nutrient budgets.

FIGURE CAPTIONS

Figure 1. Location map of Leg 167 California Margin sites.

Figure 2. Site 1010 master columns showing examples of core recovery, simplified lithology, biostratigraphic and magnetostratigraphic zonations, and GRAPE density records.

Figure 3. Age vs. depth plot for Hole 1011B.

Figure 4. Interstitial water geochemistry of Coastal Transect sites (symbols from north to south: solid square, Site 1019; solid triangle, Site 1022; solid diamond, Site 1018; solid circle, Site 1017; open square, Site 1014; open triangle, Site 1013; open diamond, Site 1012; open circle, Site 1011). Alkalinity shows interplay of organic carbon diagenesis and interactions with the sediments. Calcium and magnesium show nonconservative profiles in the upper portion from authigenic mineral formation and ion exchange reactions. Deeper profiles are often conservative (linear correlation between Ca increase and Mg decrease), suggesting primary control by the diffusive influence of reactions in the underlying basalt. Silicate values are shown vs. depth and vs. temperature. The much narrower spread of values vs. temperature suggests biogenic opal solubility with temperature as primary control on concentration of dissolved silicate.

Figure 5. Thermal gradients at Leg 167 sites.

Figure 6. Hole 1014A magnetic susceptibility log data for passes 1 and 2. Value differences between the two passes are real and reflect changes in internal tool temperature as the tool warms in the borehole, an effect that can be corrected after processing. Broad-scale susceptibilty variations (2- to 3-m scale) are very similar to the core-based susceptibility measurements and can be used for core-log correlation purposes.

Figure 7. Obtaining a composite section. Smoothed (15 cm Gaussian) GRAPE bulk density data for the upper 250 on the mcd scale. Holes 1016A (lowermost) through Hole 1016D (uppermost curve) are vertically offset from each other by a constant (0.15 g/cm^3). Cores are aligned relative to characteristic features.

Figure 8. A. Shipboard 3.5-kHz precision depth recorder (PDR) record acquired during the Site 1016 presite survey; arrow marks the location where the beacon was dropped. Changes

in **(B)** PWL velocity and **(C)** GRAPE density from Hole 1016A mapped to seismic reflectors.

Figure 9. Depth variations of **(A)** C_{37} alkenone abundance, **(B)** $U^{k'}_{37}$ value, and calculated sea-surface temperature (SST), and **(C)** total organic carbon (TOC) contents in sediments of Hole 1017B.

Figure 10. A. Predicted opal content for Hole 1018A based on site-survey reflectance and opal data. Characteristic reflectance spectra of **(B)** diatom clay with silt, **(C)** clay with silt, and **(D)** nannofossil chalk with diatoms and clay.

Figure 11. Magnetostratigraphy (after 20-mT AF demagnetization) of sediments from Site 1021 (Delgada Fan). A complete magnetostratigraphy is obtained for the past 5.2 m.y.

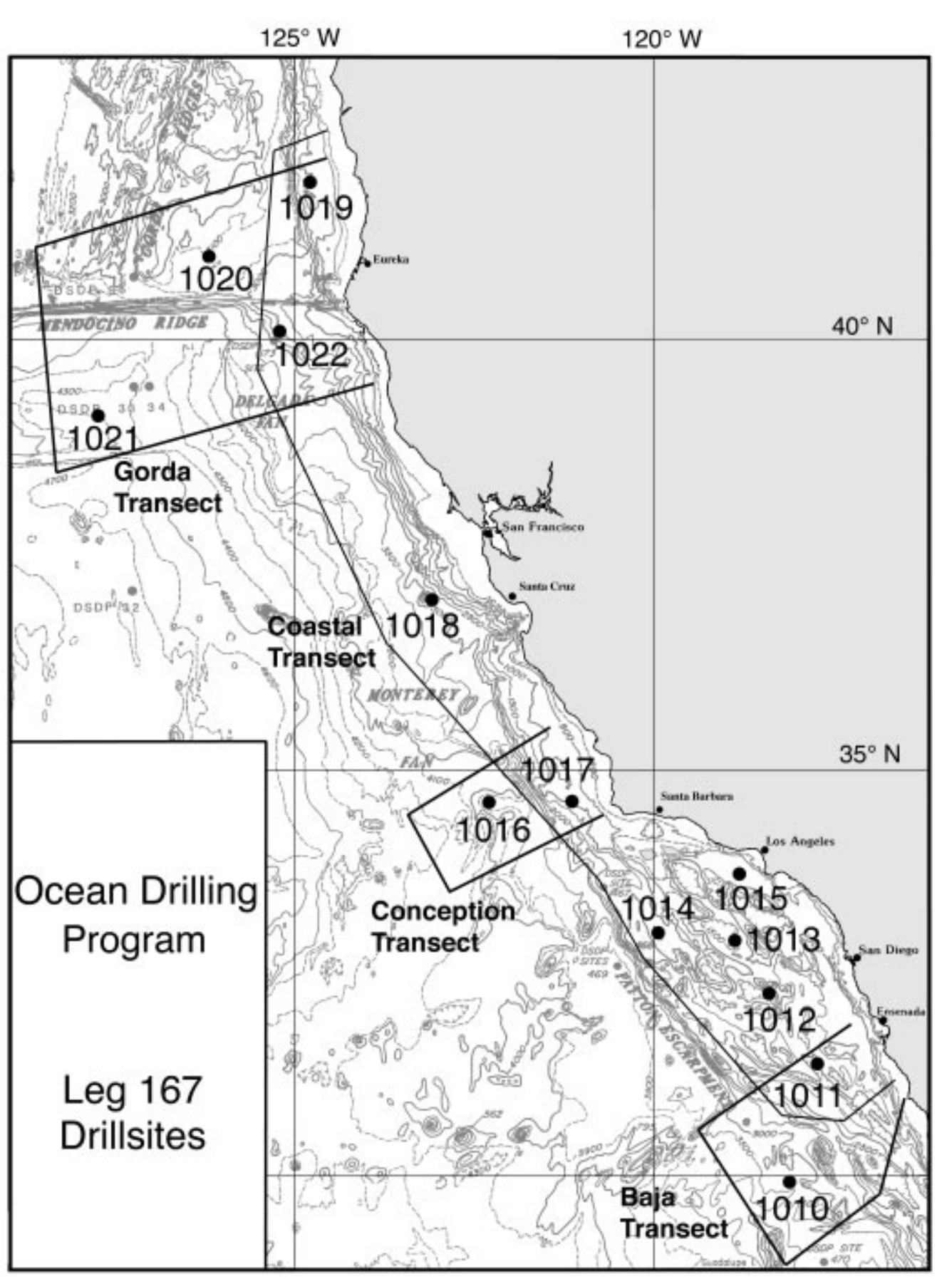
125° W
120° W
40° N
35° N
1019
1020
1022
1021
Gorda
Transect
Coastal
Transect
1018
1017
1016
Conception
Transect
1014
1015
1013
1012
1011
1010
Baja
Transect
Eureka
San Francisco
Santa Cruz
Santa Barbara
Los Angeles
San Diego
Ensenada
MENDOCINO RIDGE
MONTEREY
FAN
PATTON ESCARPMENT
DSDP
Ocean Drilling
Program
Leg 167
Drillsites

Master Column Leg 167 Site 1010

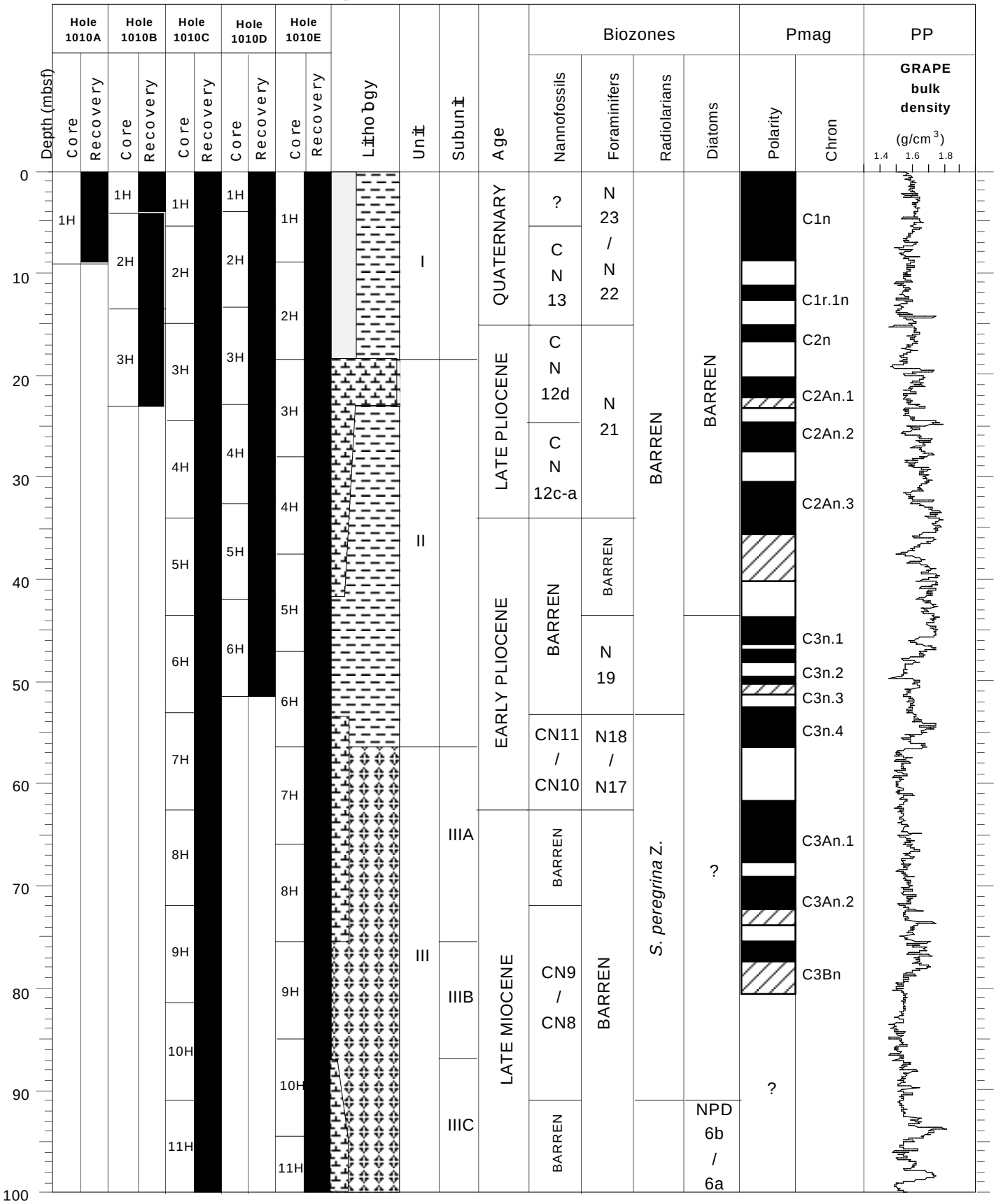

Master Column Leg 167 Site 1010

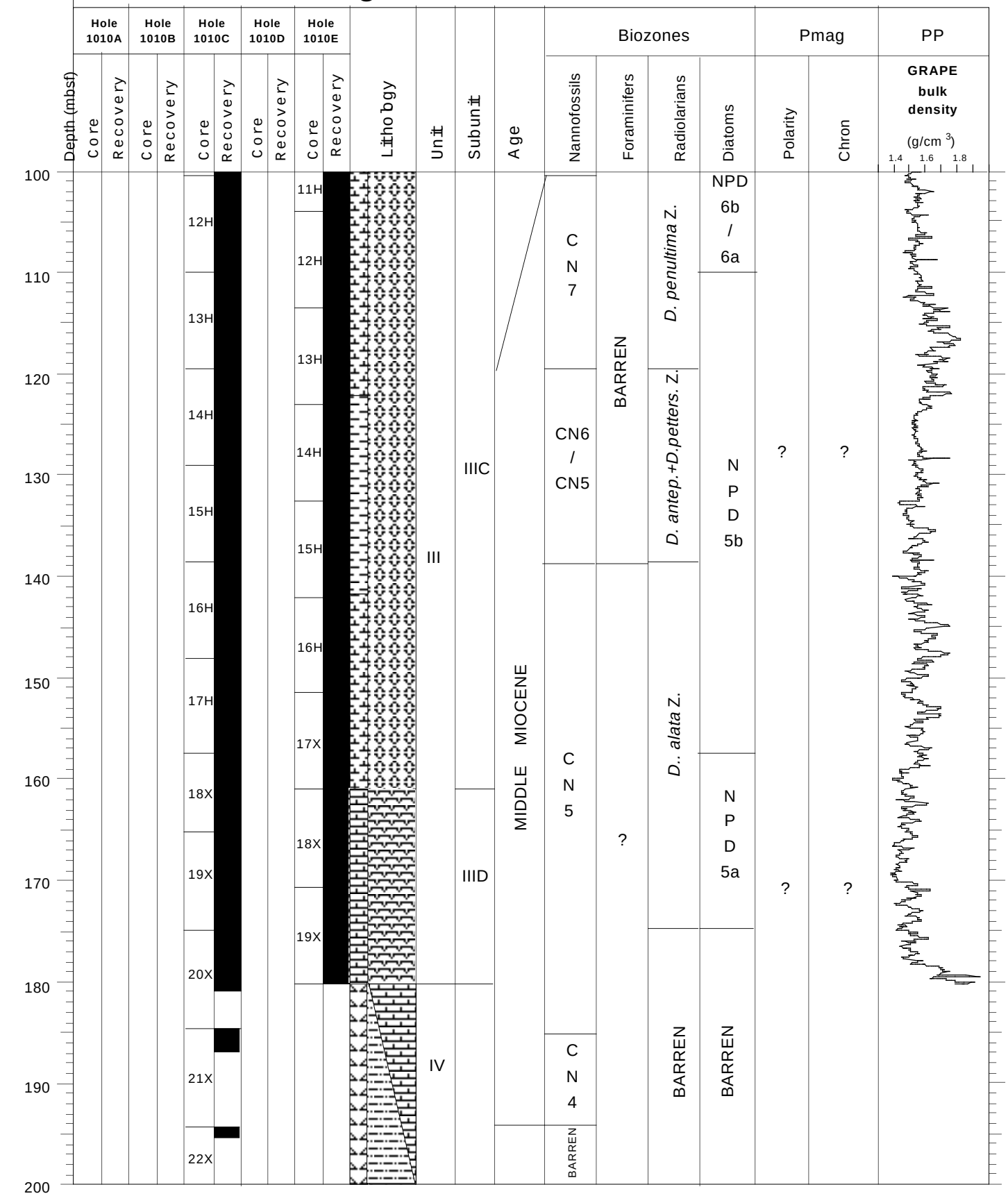

Master Column Leg 167 Site 1010

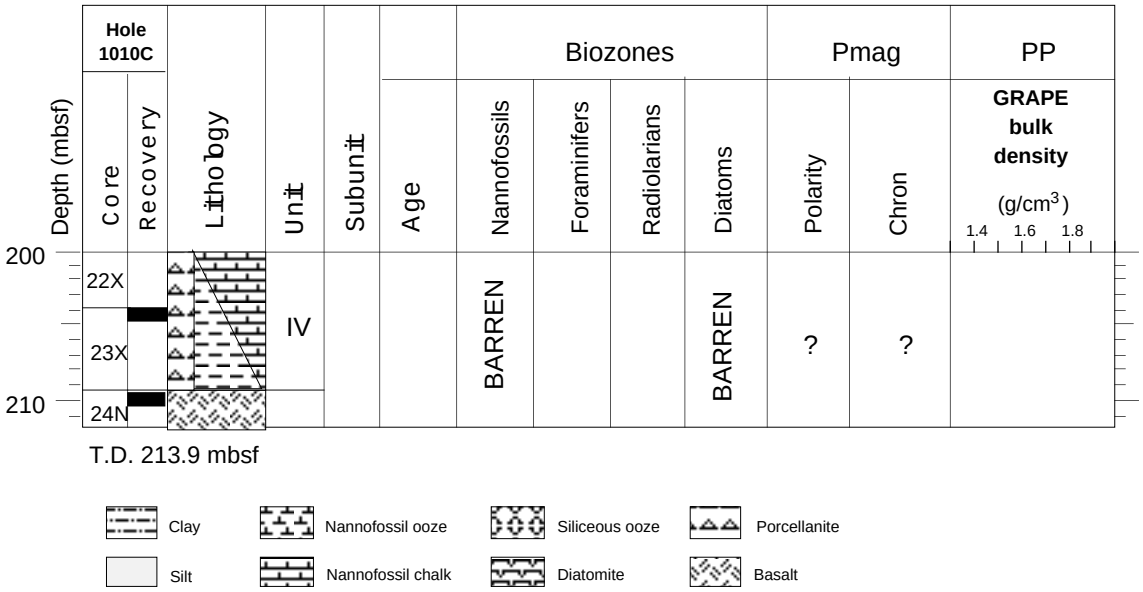

T.D. 213.9 mbsf

Clay
Silt
Nannofossil ooze
Nannofossil chalk
Siliceous ooze
Diatomite
Porcellanite
Basalt

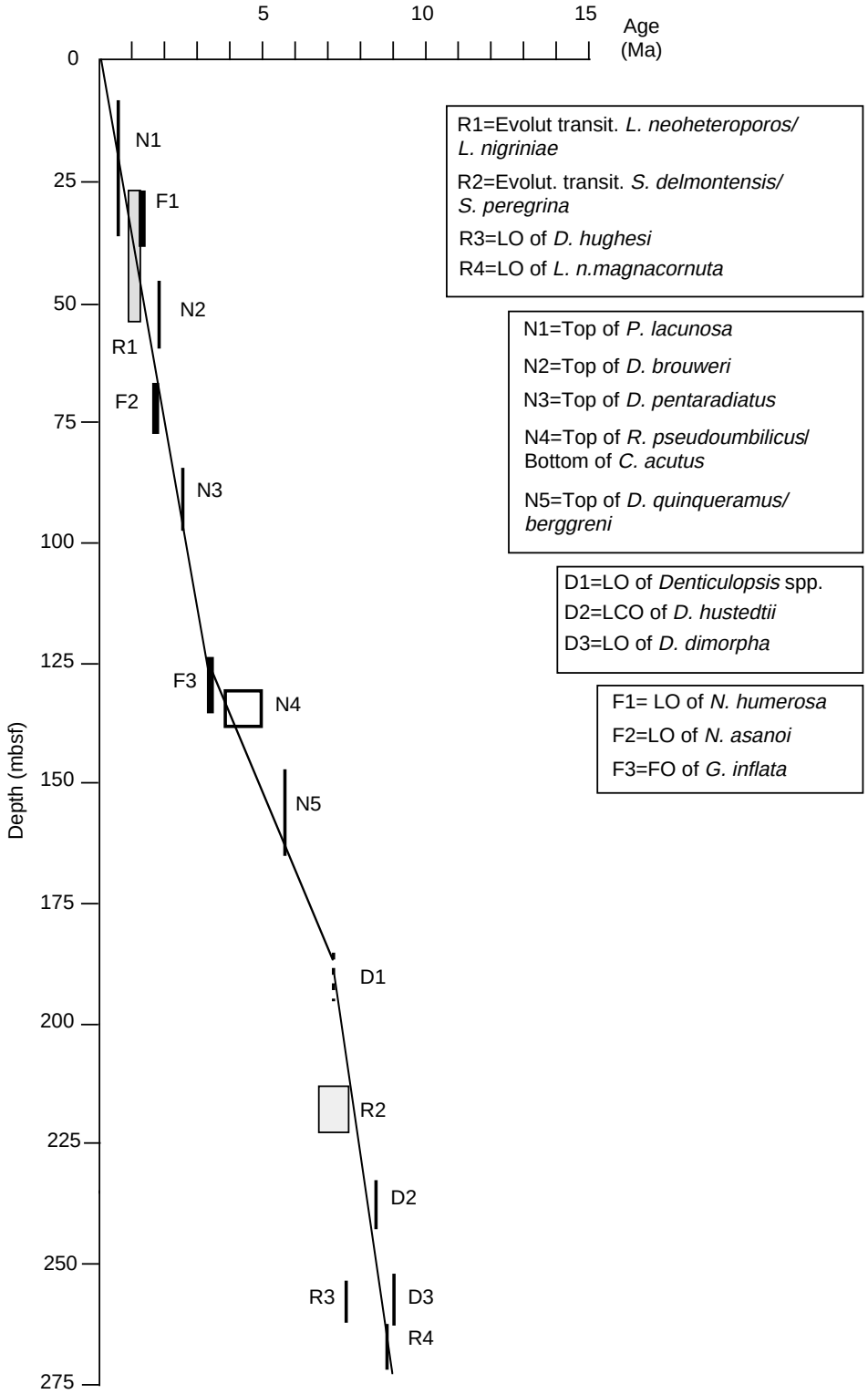
5
10
15
Age
(Ma)
0
25
50
75
100
125
150
175
200
225
250
275
Depth (mbsf)
N1
F1
N2
R1
F2
N3
F3
N4
N5
D1
R2
D2
R3
D3
R4
R1=Evolut transit. L. neoheteroporos/ L. nigriniae
R2=Evolut. transit. S. delmontensis/ S. peregrina
R3=LO of D. hughesi
R4=LO of L. n.magnacornuta
N1=Top of P. lacunosa
N2=Top of D. brouweri
N3=Top of D. pentaradiatus
N4=Top of R. pseudoumbilicus/ Bottom of C. acutus
N5=Top of D. quinqueramus/ berggreni
D1=LO of Denticulopsis spp.
D2=LCO of D. hustedtii
D3=LO of D. dimorpha
F1= LO of N. humerosa
F2=LO of N. asanoi
F3=FO of G. inflata

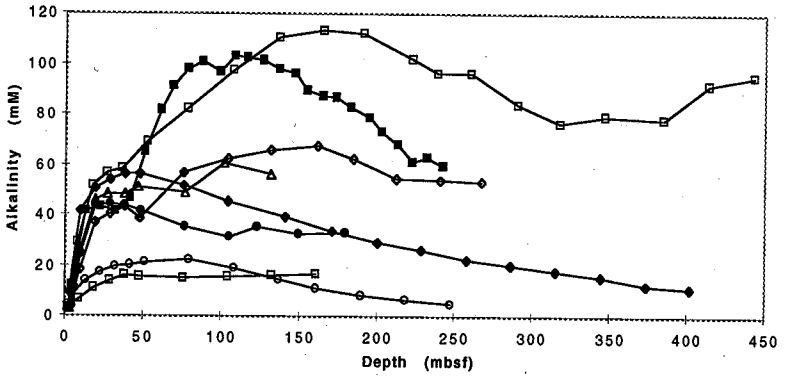
Alkalinity (mM)
Depth (mbsf)

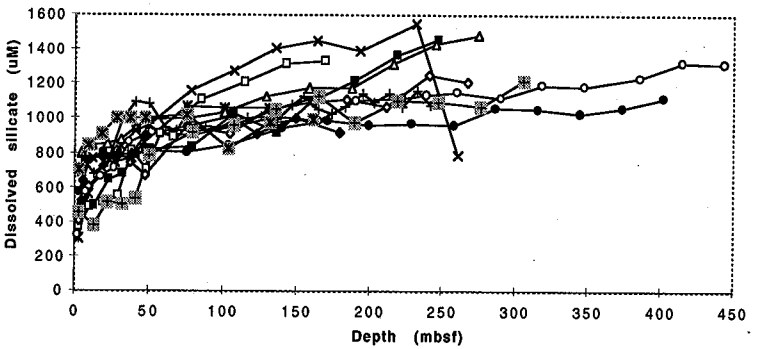
Dissolved silicate (uM)
Depth (mbsf)

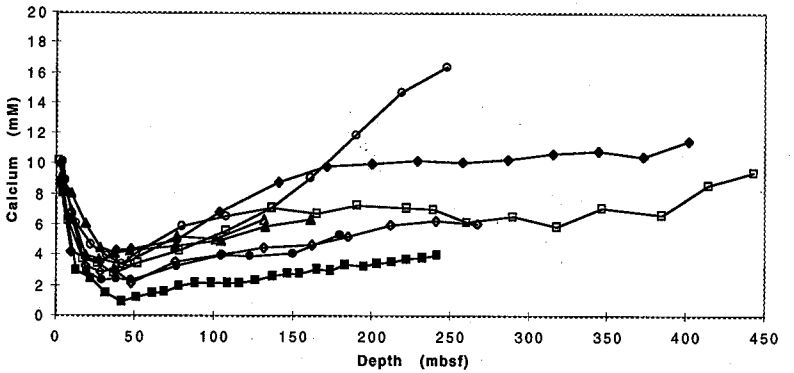
Calcium (mM)
Depth (mbsf)

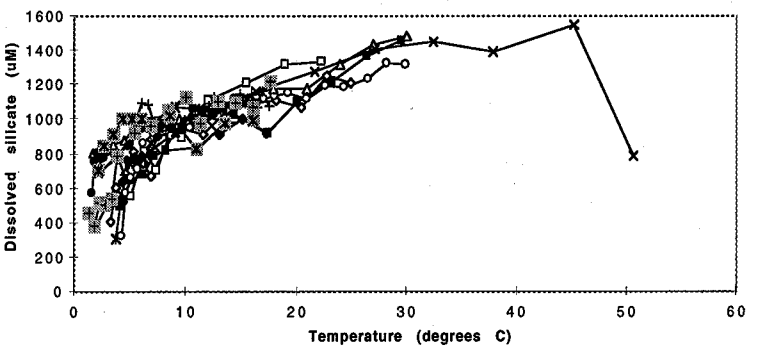
Dissolved silicate (uM)
Temperature (degrees C)

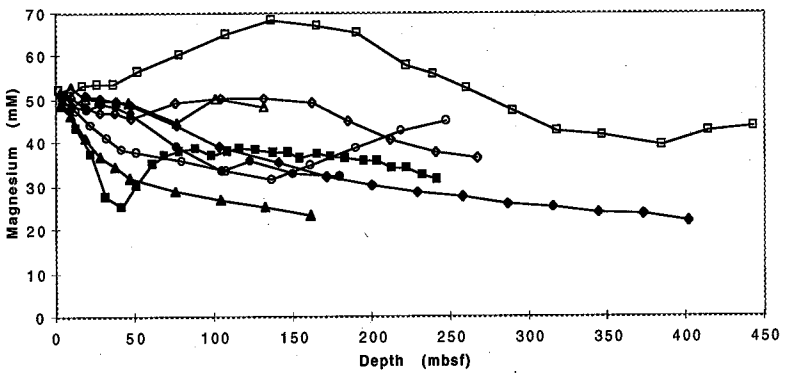
Magnesium (mM)
Depth (mbsf)

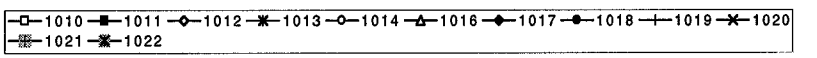
1010
1011
1012
1013
1014
1016
1017
1018
1019
1020
1021
1022

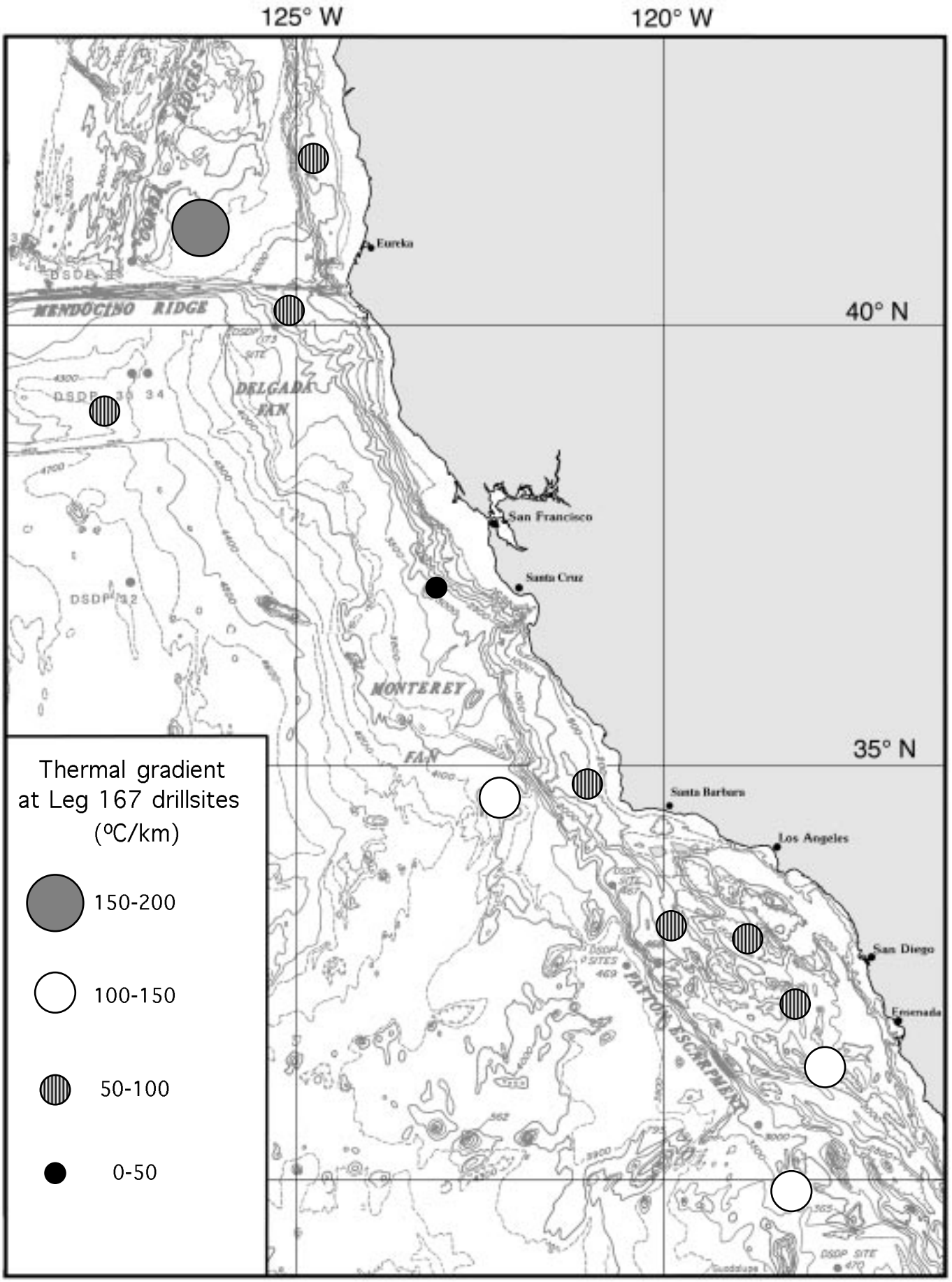
125° W
120° W
40° N
35° N
Eureka
MENDOCINO RIDGE
DELGADA FAN
San Francisco
Santa Cruz
MONTEREY FAN
Santa Barbara
Los Angeles
San Diego
Ensenada
PATTON ESCARPMENT
Thermal gradient at Leg 167 drillsites (ºC/km)
150-200
100-150
50-100
0-50

Hole 1014A

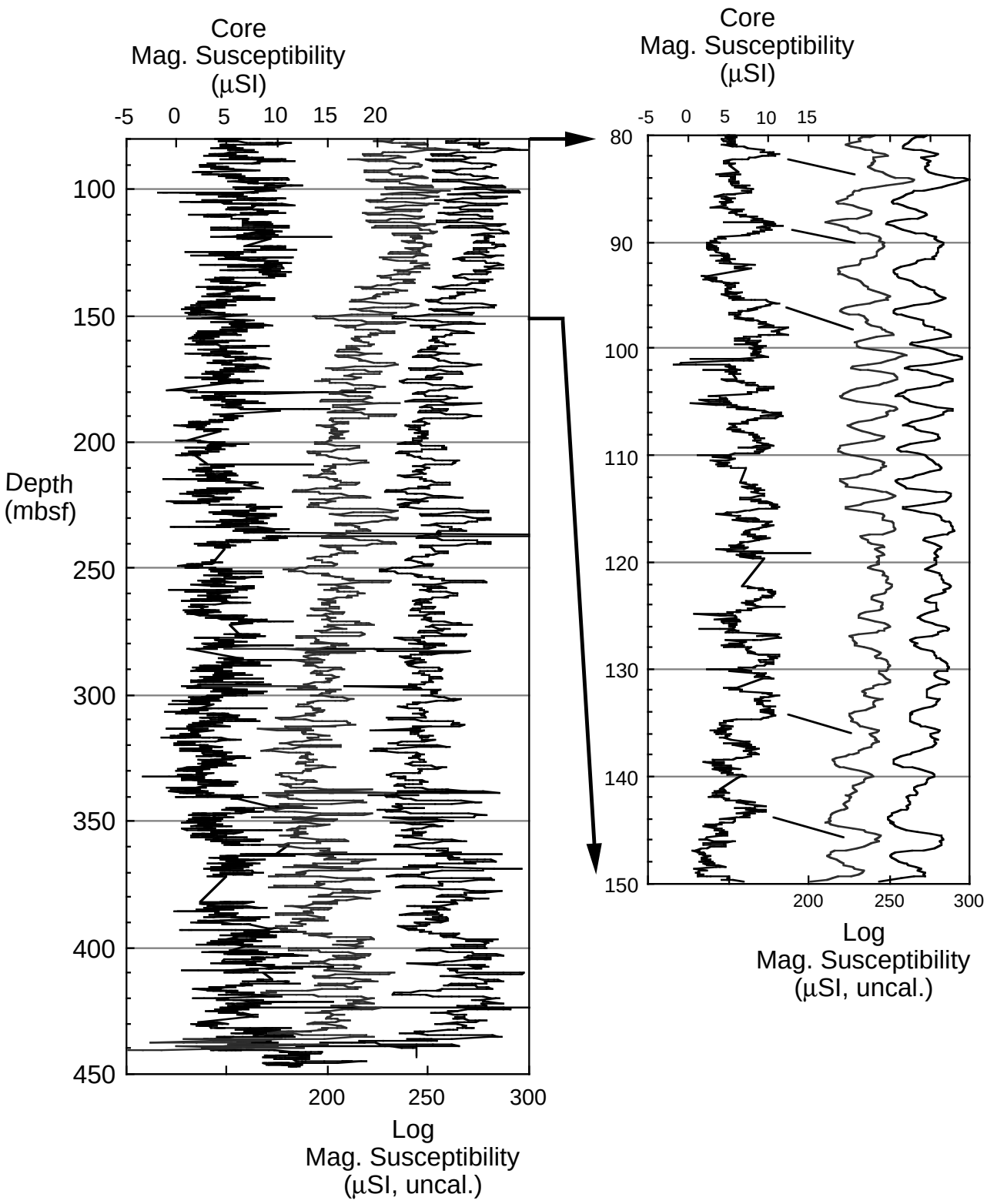
Core
Mag. Susceptibility
(μSI)
-5 0 5 10 15 20
100
150
200
250
300
350
400
450
Depth
(mbsf)
200 250 300
Log
Mag. Susceptibility
(μSI, uncal.)
Core
Mag. Susceptibility
(μSI)
-5 0 5 10 15
80
90
100
110
120
130
140
150
200 250 300
Log
Mag. Susceptibility
(μSI, uncal.)

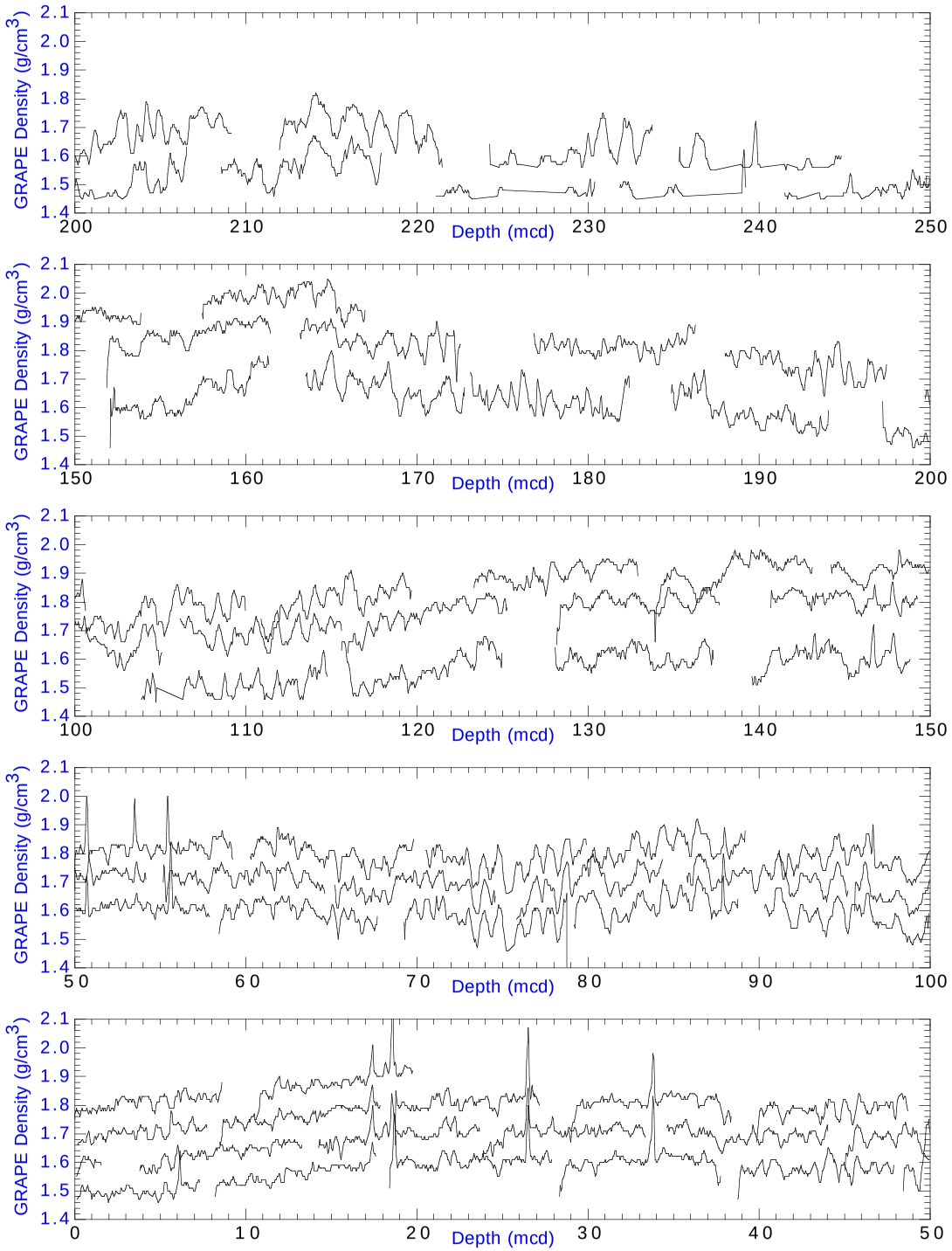
GRAPE Density (g/cm3)
2.1
2.0
1.9
1.8
1.7
1.6
1.5
1.4
200
210
220
230
240
250
Depth (mcd)
150
160
170
180
190
200
100
110
120
130
140
150
50
60
70
80
90
100
0
10
20
30
40
50

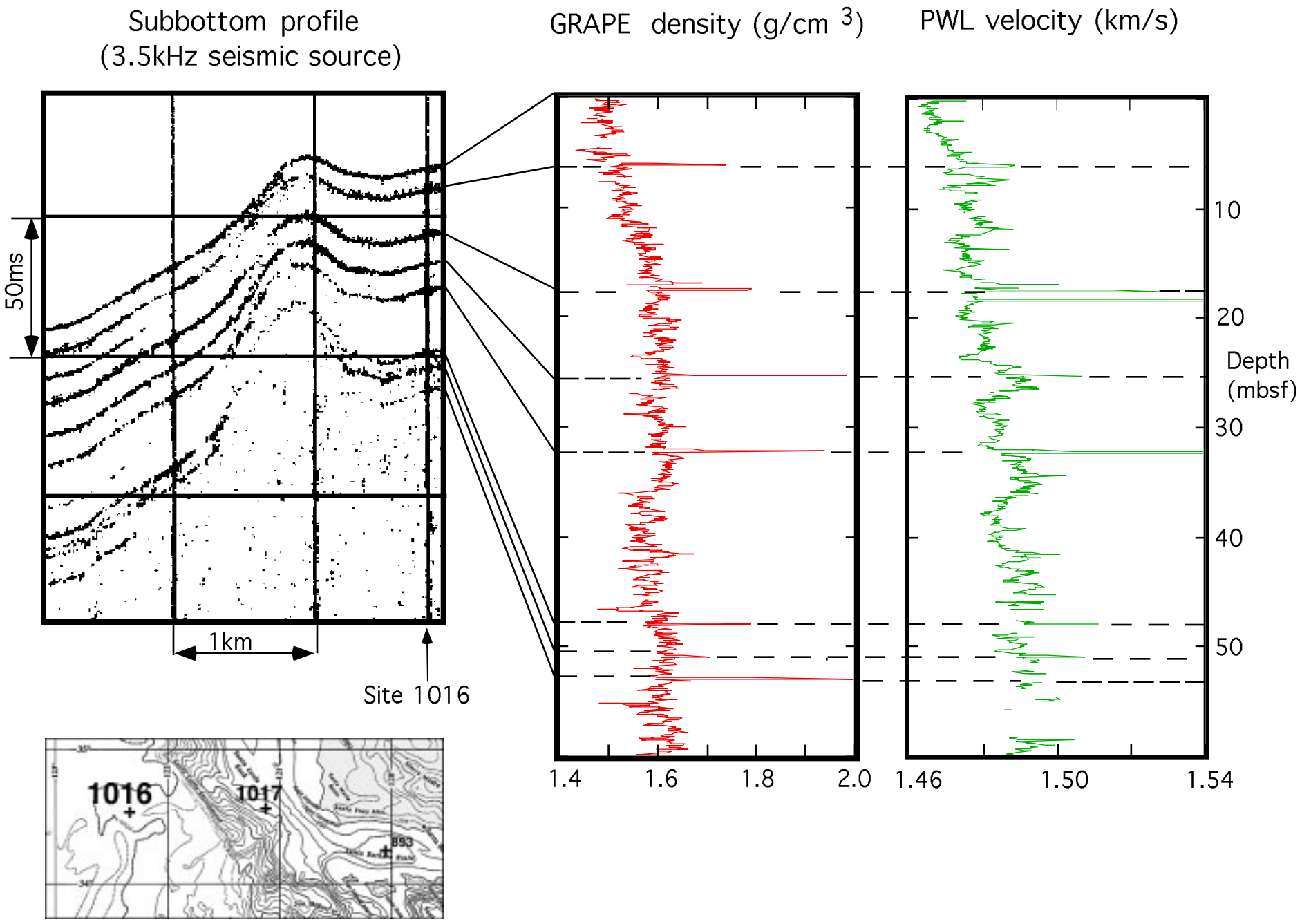
Subbottom profile
(3.5kHz seismic source)
GRAPE density (g/cm 3)
PWL velocity (km/s)
50ms
1km
Site 1016
1016
1017
893
1.4
1.6
1.8
2.0
1.46
1.50
1.54
10
20
30
40
50
Depth
(mbsf)

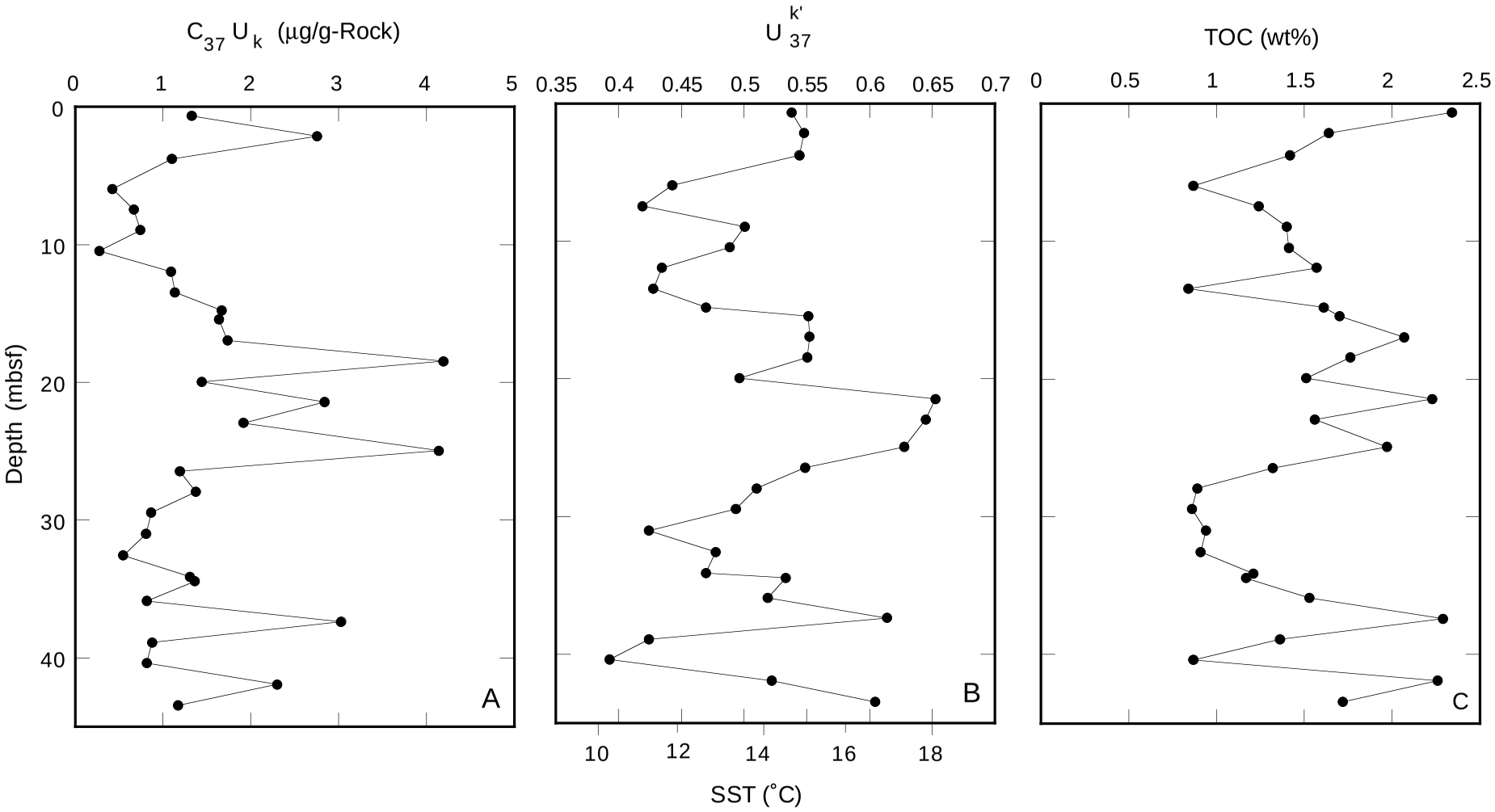
$C_{37} U_k$ (µg/g-Rock)
0
1
2
3
4
5
Depth (mbsf)
0
10
20
30
40
A
$U^{k'}_{37}$
0.35
0.4
0.45
0.5
0.55
0.6
0.65
0.7
B
10
12
14
16
18
SST (˚C)
TOC (wt%)
0
0.5
1
1.5
2
2.5
C

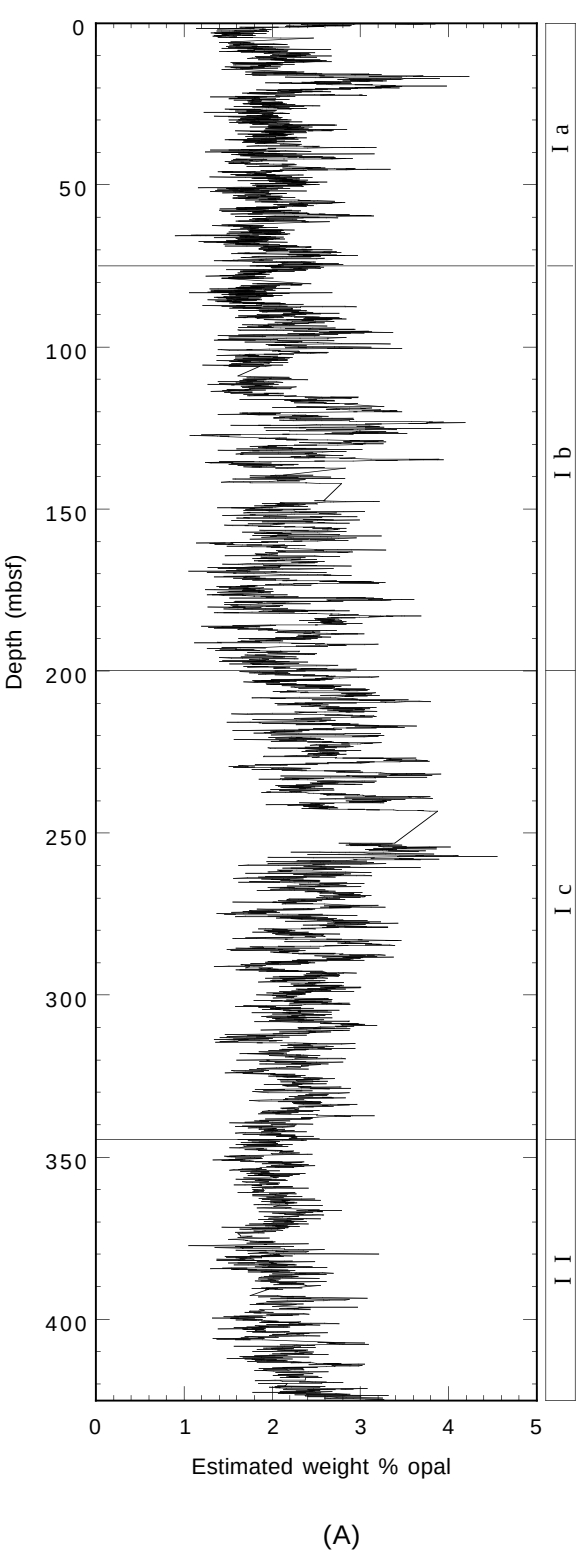
Depth (mbsf)
0
50
100
150
200
250
300
350
400
I a
I b
I c
I I
0
1
2
3
4
5
Estimated weight % opal

(A)

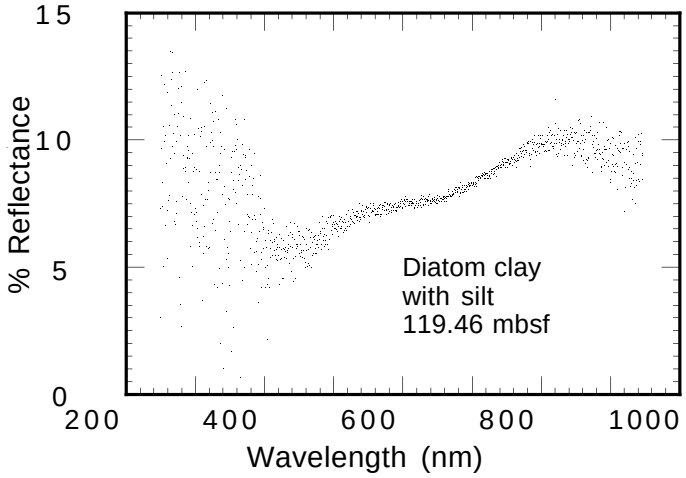
% Reflectance
15
10
5
0
Diatom clay
with silt
119.46 mbsf
200
400
600
800
1000
Wavelength (nm)

(B)

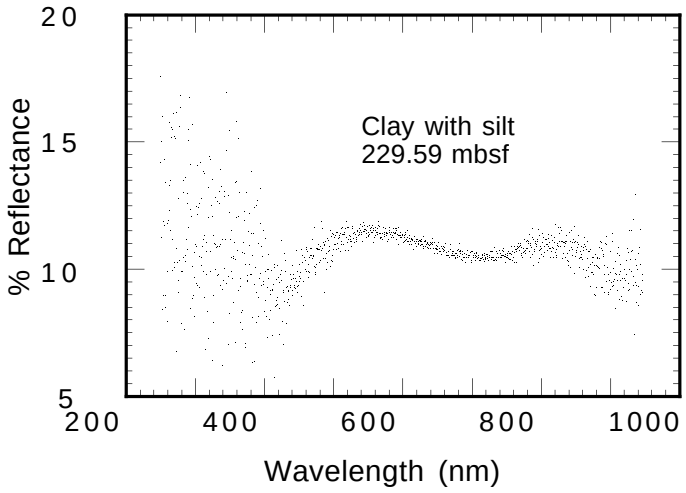
% Reflectance
20
15
10
5
Clay with silt
229.59 mbsf
200
400
600
800
1000
Wavelength (nm)

(C)

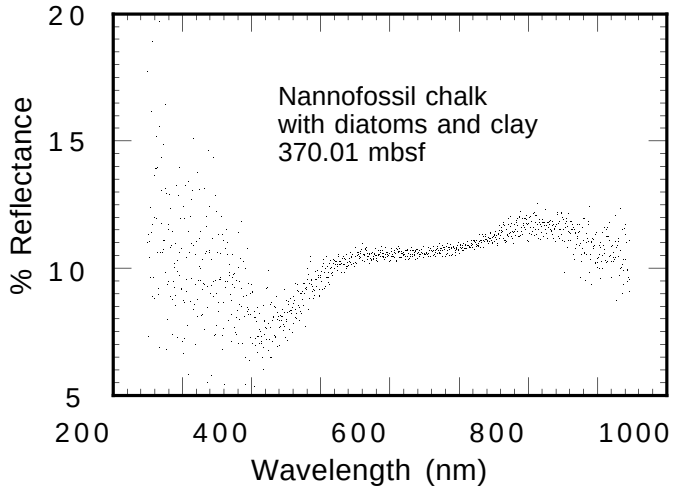
% Reflectance
20
15
10
5
Nannofossil chalk
with diatoms and clay
370.01 mbsf
200
400
600
800
1000
Wavelength (nm)

(D)

Magnetostratigraphy of sediments from the outer Delgada fan

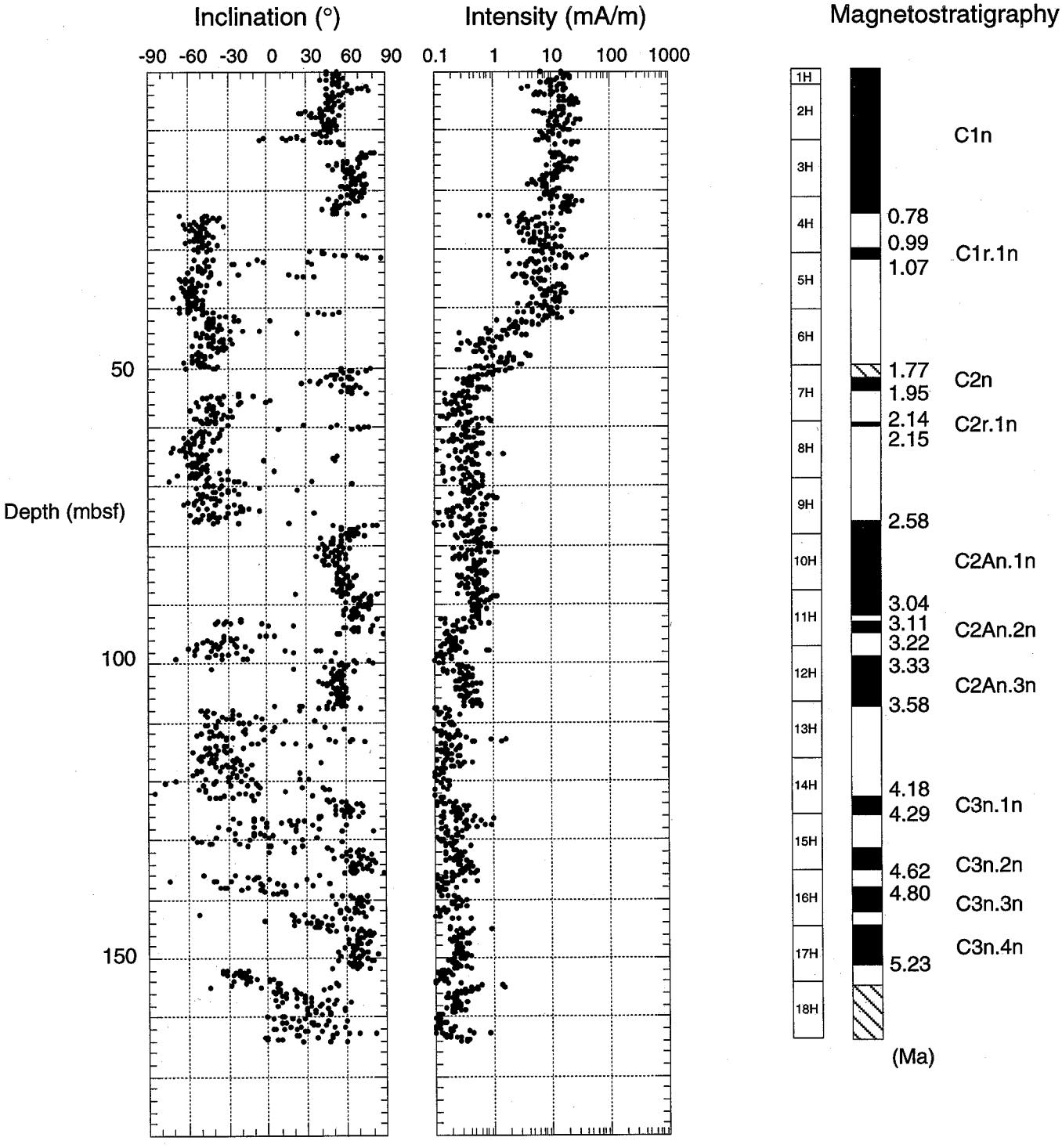

OPERATIONS REPORT

The ODP Operations and Engineering personnel aboard *JOIDES Resolution* for Leg 167 were

Operations Manager: Scott McGrath

Schlumberger Engineer:Raymond Faust

Leg 167 Operations were highly successful and met or exceeded all scientific objectives. Two new ODP records were set during the leg, with a total of 7501.54 m of core recovered and 52 holes drilled. The overall core recovery percentage for the leg was 97.3% for 840 cores over 13 sites. Outstanding results were obtained from both the advanced piston coring (APC) and extended core barrel (XCB) coring systems during the leg. The motor driven core barrel (MDCB) was also deployed successfully to obtain a fresh basalt sample at the conclusion of an APC/XCB hole. A total of 7 different sites were logged with excellent results obtained from the Triple Combination (density, neutron porosity, resistivity, and natural gamma ray), Formation MicroScanner (FMS), and Geological High-Sensitivity Magnetic Tool (GHMT) strings. The Adara temperature tool was deployed 44 times, obtaining 40 good data points.

A subsea television camera survey was run at two different sites: Site 1016 (proposed Site CA-11E) and Site 1018 (proposed Site CA-8A). Site 1016 was 5 nmi outside a former chemical munitions dumping area, and Site 1018 was 7 nmi outside of a former explosives dumping area. The survey at Site 1016 was negative, and coring proceeded normally. A small round artifact was discovered at Site 1018, the vessel was offset 150 m, and another survey was conducted with negative results allowing coring to commence normally. An examination of the first two cores at both sites was conducted with normal results.

A half-day port call was made in San Diego, California, on 7 May to unload approximately 1500 m of core. The port call was planned before the leg because the pre-leg estimate of 7300 m of core recovered exceeded the capacity of 6200 m for the refrigerated storage on board the vessel.

A rendezvous with a small boat from the University of California, Santa Barbara (UCSB), occurred in the Santa Barbara channel on 12 May. The rendezvous allowed 5 small boxes of core to be sent to UCSB for immediate isotope analysis and biostratigraphy studies.

TRANSIT FROM ACAPULCO TO SITE 1010

The 1346 nmi transit from Acapulco to Site 1010 (proposed Site CA-14A) was accomplished in 119 hr at an average speed of 11.3 kt. A 3.5-kHz precision depth recorder (PDR) survey was performed while approaching the site. A Datasonics 354M beacon was dropped on Global Positioning System (GPS) coordinates at 1045 hr (local time = GMT – 7) on 25 April.

SITE 1010 (PROPOSED SITE CA-14A)

Hole 1010A

Hole 1010A was spudded at 1845 hr on 25 April with an APC/XCB/MDCB coring assembly. A single APC core (Core 167-1010A-1H) was taken from 0 to 9.5 meters below seafloor (mbsf). A full barrel prevented the establishment of an accurate mudline and the hole was abandoned.

Hole 1010B

The drill pipe was raised 4 m and Hole 1010B was spudded at 1945 hr on 25 April. The water depth was established at 3475.3 meters below rig floor (mbrf) based on recovery of the mudline core. APC Cores 167-1010B-1H through 3H were taken from 0 to 23.2 mbsf with 102.2% recovery. A sudden power failure in the auxiliary 480-V transformer temporarily caused a generator to drop offline. The drill pipe was pulled above the seafloor, ending Hole 1010B while repairs were made to the generator.

Hole 1010C

The vessel was offset 10 m to the north and Hole 1010C was spudded at 0200 hr on 26 April. The water depth was established at 3476.5 mbrf based on recovery of the mudline core. APC Cores 167-1010C-1H through 17H were taken from 0 to 157.5 mbsf with

103.9% recovery. Oriented cores were obtained starting with Core 3H. XCB Cores 18X through 23X were taken down to 209.4 mbsf with 55% recovery. Excellent recovery was obtained on XCB Cores 18X through 20X, but a chert layer found on Core 21X broke off several of the tungsten carbide inserts on the XCB cutting shoe, resulting in a jammed core liner. The inserts were recovered in the core catcher. XCB Cores 22 through 23X were taken with a carbonado diamond shoe. Core 22X suffered from core jamming, and Core 23X penetrated basalt, and was terminated after 5.6 m advancement in 45 min. One MDCB core was taken down to 213.9 mbsf, and a solid section of basalt was recovered (cored 4.5 m, recovered 0.91 m).

Hole 1010D

Hole 1010D was spudded at 0600 hr on 27 April. The water depth was established at 3477.5 mbrf. APC Cores 167-1010D-1H through 6H were taken from 0 to 51.5 mbsf with 106% recovery. Adara heat-flow measurements were performed on Cores 3H through 6H. Following Core 6H, the coring wireline became wrapped around the sinker bar assembly, trapping the core barrel in the BHA. Attempts to free the core barrel were unsuccessful. The Kinley cutter was dropped, and the coring line was sheared immediately above the core barrel allowing the coring line to be retrieved. The drill string was pulled clear of the seafloor at 1645 hr on 27 April.

Hole 1010E

After pulling the drill pipe and bottom-hole assembly (BHA) to the surface, the core barrel was dislodged from the BHA, and the pipe was tripped back to bottom. Hole 1010E was spudded at 0430 on 28 April. The water depth was established at 3476.5 mbrf. APC Cores 167-1010E-1H through 16H were taken from 0 from 151.5 mbsf with 103.1% recovery). XCB Cores 17X to 19X were taken to 180.2 mbsf with 100.1% recovery. The pipe was pulled clear of the seafloor at 2200 hr 28 April, ending Hole 1010E.

Hole 1010F

The vessel was offset 10 m to the south and Hole 1010F was spudded at 2300 hr 28 April. The water depth was established at 3476.3 mbrf. APC Cores 1H through 6H were taken down to 55.7 mbsf with 102.3% recovery. The drill string was tripped back to the surface and secured for the 8-hr transit to Site 1011 by 0945 29 April.

SITE 1011 (PROPOSED SITE CAM-2A)

Site 1010 to Site 1011

The 82.5-nmi transit from Site 1011 to Site 1011 (proposed Site CAM-2A) was accomplished in 7.5 hr at an average speed of 11.5 kt. A 3.5-kHz PDR survey was performed while approaching Site 1011. A Datasonics 354M beacon was dropped on GPS coordinates at 1715 hr on 29 April.

Hole 1011A

Hole 1011A was spudded, and a single APC core (Core 167-1011A-1H) was taken from 0 to 9.5 mbsf. A full barrel prevented the establishment of an accurate mudline, and the hole was abandoned.

Hole 1011B

The drill pipe was raised 3 m, and Hole 1011B was spudded at 2245 hr on 29 April. The water depth was established at 2032.5 mbrf based on recovery of the mudline core. APC Cores 1671011B-1H through 15H were taken from 0 to 137.9 mbsf with 103.8% recovery. XCB Cores 16X through 31X were taken down to 281.5 mbsf with 89.1% recovery. Hole 1011B was terminated after recovery of several sections of vesicular basalt. A wiper trip was made from 281.5 mbsf up to 78 mbsf and back to the bottom of the hole where 3 m of fill was found. The pipe was raised to 78.5 mbsf and preparations for logging were made. Hole 1011B was logged with the Triple Combination tool string (density, neutron porosity,

resistivity, and natural gamma ray) from 2310 to 2113 mbrf (277.5 to 79.5 mbsf). The FMS/Sonic/Gamma Ray (GR) tool string was run from 2310 to 2128 mbrf (277 to 95 mbsf). Both logging runs obtained excellent results. The pipe was pulled clear of the seafloor at 1830 hr 1 May, ending Hole 1011B.

Hole 1011C

Hole 1011C was spudded at 1900 hr on 1 May. APC Cores 167-1011C-1H through 15H were taken from 0 to 136.6 mbsf with 103.8% recovery. XCB Cores 1011C-16X through 20X were taken down to 184.2 mbsf with 101.2% recovery. The pipe was pulled clear of the seafloor at 1215 hr 2 May, ending Hole 1011C.

Hole 1011D

Hole 1011D was spudded at 1245 hr on 2 May. APC Cores 167-1011D-1H and 2H were taken from 0 to 16.9 mbsf with 102% recovery. The pipe was pulled clear of the seafloor at 1330 hr 2 May, ending Hole 1011D.

Hole 1011E

Hole 1011E was spudded at 1345 on 2 May. APC Cores 1011E-1H through 16H were taken down to 142.3 mbsf with 104.4% recovery. The drill string was tripped back to the surface and cleared the rotary table at 0130 hr 3 May, ending Hole 1011E. The *JOIDES Resolution* was underway for the 7.5-hr transit to Site 1012 by 0145 hr 3 May.

SITE 1012 (PROPOSED SITE BA-1)

Transit from Site 1011 to Site 1012

The 69.0-nmi transit from Site 1011 to Site 1012 (proposed Site BA-1) was accomplished in 5.75 hr at an average speed of 11.5 kt. A 3.5-kHz PDR survey was performed while approaching Site 1012. A Datasonics 354M beacon was dropped on GPS coordinates at 0800 hr on 3 May.

Hole 1012A

Hole 1012A was spudded at 1145 hr on 3 May. APC Cores 167-1012A-1H through 13H were taken from 0 to 118.7 mbsf with 105.7% recovery. Oriented cores were obtained starting with Core 3H. XCB Cores 14X through 30X were taken to 273.5 mbsf with 93.2% recovery. Headspace methane concentration increased with increasing depth, but no significant higher weight molecular hydrocarbons other than C1 and C2 were observed, indicating that the methane is of biogenic origin and not significant for safety and pollution investigations. The hole was displaced with heavy mud at the completion of coring operations.

Hole 1012B

Hole1012B was spudded at 1530 hr on 4 May. APC Cores 167-1012B-1H through 14H were taken from 0 to 132.3 mbsf with 99.2% recovery. Adara temperature measurements were taken on Cores 4H, 6H, 8H, and 10H.

Hole 1012C

Hole 1012C was spudded at 0115 hr on 5 May. APC Cores 167-1012C-1H through 9H were taken down to 82.6 mbsf with 105.2% recovery. The drill string was tripped back to the surface and secured for the 3.25-hr transit to Site 1013 by 0945 hr on 5 May.

SITE 1013 (PROPOSED SITE BA-2B)

Transit from Site 1012 to Site 1013

The 38.0-nmi transit from Site 1012 to Site 1013 (proposed Site BA-2B) was accomplished in 3.25 hr at an average speed of 11.7 kt. The *JOIDES Resolution* arrived at Site 1013 at 1345 hr on 5 May. A 3.5-kHz PDR survey was performed while approaching Site 1013. A Datasonics 354M beacon was dropped on GPS coordinates at 1345 hr on 5 May.

Hole 1013A

Hole 1013A was spudded at 1730 hr on 5 May. APC Cores 167-1013A-1H through 10H were taken from 0 to 90.6 mbsf with 100.8% recovery. Oriented cores were obtained starting with Core 3H. XCB Cores 11X through 16X were taken to 146.1 mbsf with 82.2% recovery.

Hole 1013B

Hole 1013B was spudded at 0730 hr on 6 May. APC Cores 167-1013B-1H through 10H were taken from 0 to 94.1 mbsf with 104.8% recovery. XCB Core 167-1013B-11X was taken down to 103.8 mbsf with 96.8% recovery. Hole 1013B was originally scheduled to penetrate to 150 mbsf, but was cut short because of the constraint of having to arrive in San Diego at 0500 hr on 7 May.

Hole 1013C

Hole 1013C was spudded at 1430 hr 6 May. APC Cores 167-1013C-1H through 8H were taken down to 72.2 mbsf with 102.4% recovery. Adara temperature measurements were taken on Cores 4H, 6H, and 8H. The time for Site 1013 expired and the drill string was tripped back to the surface and secured for the 8-hr transit to San Diego by 2115 hr 6 May.

SITE 1014 (PROPOSED SITE CA-15A)

Transit from San Diego to Site 1014

The 151.0-nmi transit from San Diego to Site 1014 (proposed Site CA-15A) was accomplished in 15.5 hr at an average speed of 10.4 kt. A 3.5-kHz PDR survey was performed while approaching the site. The *JOIDES Resolution* arrived at Site 1014 at 0530 hr on 8 May.

Hole 1014A

Hole 1014A was spudded at 0900 hr on 8 May. APC Cores 167-1014A-1H through 6H

were taken from 0 to 50.6 mbsf with 100.8% recovery. Oriented cores were obtained starting with Core 3H. APC refusal was reached at 50.6 mbsf when 70,000 lb of overpull was required to free the barrel. XCB Cores 7X through 50X were taken down to 449.0 mbsf with 88.7% recovery. Hole 1014A was logged with the Triple Combination, the FMS/Sonic/GR, and the GHMT tool strings from 443 to 58 mbsf with good results. The vessel was offset 100 m to the east in an attempt to find an area more conducive to APC coring.

Hole 1014B

Hole 1014B was spudded at 1915 hr on 10 May. APC Cores 167-1014B-1H through 13H were taken from 0 to 114.7 mbsf with 100.8% recovery. Apparently, the 100-m offset was enough to allow the piston coring to continue deeper than at Hole1014A before APC refusal. Adara temperature measurements were taken on Cores 3H through 6H and on Core 8H, and three good data points were acquired. While pulling the core liner from the core barrel following Core 13H, the first meter of the liner exploded. The remaining liner was still inside the core barrel and shattered, but remained intact enough to be pulled out of the core barrel. The portion of the liner that exploded caused part of the core to fall on the rig floor. XCB coring continued with Cores 167-1014B-14X through 27X, and was taken down to 245.0 mbsf with 83.6% recovery.

Hole 1014C

Hole 1014C was spudded at 1315 hr on 11 May. APC Cores 167-1014C-1H and 2H were taken down to 19.5 mbsf with 102.8% recovery.

Hole 1014D

Hole 1014D was spudded at 1400 hr on 11 May. APC Cores 167-1014D-1H through 10H were taken down to 92.0 mbsf with 104.5% recovery. XCB Cores 167-1014D-11X through 13X were taken down to 120.9 mbsf with 83.8% recovery. The drill string was tripped back to the surface and secured for the 8-hr transit to Site 1015 by 2145 hr on 11 May.

SITE 1015 (PROPOSED SITE BA-4D)

Transit from Site 1014 to Site 1015

The 85.0-nmi transit from Site 1014 to Site 1015 (proposed Site BA-4D) was accomplished in 7.75 hr at an average speed of 11.0 kt. A 3.5-kHz PDR survey was performed while approaching Site 1015. The *JOIDES Resolution* arrived at Site 1015 at 0530 hr on 12 May.

Hole 1015A

Hole 1015A was spudded at 0815 hr on 12 May. APC Cores 167-1015A-1H through 16H were taken from 0 to 149.5 mbsf with 93.1% recovery. Oriented cores were obtained on Cores 3H through 9H. An Adara temperature measurement was run on Core 4H. Further Adara measurements were canceled because of overpull and the slow drilling advancement. Advancement of the APC bit was very slow through the entire APC sequence. The recovered core exhibited multiple turbidites, which contributed to the slow drilling conditions. The vessel was offset 100 m to the east in an attempt to find an area more conducive to APC coring.

Hole 1015B

Hole 1015B was spudded at 2000 hr on 12 May. APC Cores 167-1015B-1H through 12H were taken from 0 to 97.8 mbsf with 83.2% recovery. The APC coring system encountered refusal in Core 12H, and the hole was terminated. The drill string was tripped back to the surface and secured for the 16-hr transit to Site 1016 by 0545 hr on 13 May.

SITE 1016 (PROPOSED SITE CA-11E)

Transit from Site 1015 to Site 1016

The 190.0-nmi transit from Site 1015 to Site 1016 (proposed Site CA-11E) was accomplished in 16.75 hr at an average speed of 11.3 kt. A rendezvous with a small vessel from UCSB occurred at 1045 hr on 13 May in the Santa Barbara channel. Five boxes of samples were offloaded to the rendezvous boat for transport to UCSB. The *JOIDES Resolution* continued on and arrived at Site 1016 at 2230 hr on 13 May.

Hole 1016A

Site 1016 is located approximately 7 nmi outside of a former chemical munitions dumping area. A subsea camera survey of the seafloor was conducted for safety reasons within a 50-m perimeter of the positioning beacon. The results of the camera survey were negative and Hole 1016A was spudded at 1600 hr on 14 May. APC Cores 167-1016A-1H through 10H were taken from 0 to 93.1 mbsf with 104.3% recovery. Cores 1H and 2H were run through the MST and then split open to search for artifacts. The search results were negative, and APC coring proceeded. Adara temperature measurements were taken on Cores 4H, 6H, and 8H. XCB Cores 11X through 35X were taken down to 315.5 mbsf with 92.5% recovery. Drilling was slow in a massive chert and porcellanite layer starting at approximately 298 mbsf. One MDCB Core 167-1016A-36N was taken down to 316.5 mbsf with 1 m of advancement and 0.44 m of chert recovered. Because of the slow progress from 298 to 316 mbsf with only fragments of chert recovered, the decision was made to stop coring at 316 mbsf and log the hole before reaching the planned depth of 440 mbsf. Hole 1016A was logged with the Triple Combination, the FMS/Sonic/GR, and the GHMT tool strings from 313 to 60 mbsf with good results.

HOLE 1016B

The vessel was offset 10 m to the west and Hole 1016B was spudded at 0800 hr on 17 May.

APC Cores 167-1016B-1H through 23H were taken from 0 to 210.8 mbsf with 103.5% recovery. Oriented cores were obtained starting with Core 3H.

HOLE 1016C

The vessel was offset 10 m to the west and Hole 1016C was spudded at 1140 hr on 18 May. APC Cores 167-1016C-1H and 2H were taken down to 18.7 mbsf with 100.3% recovery.

Hole 1016D

Hole 1016D was spudded at 1315 hr on 18 May. APC Cores 167-1016D-1H through 16H were taken down to 150.5 mbsf with 102.8% recovery. The drill string was tripped back to the surface and secured for the 5-hr transit to Site 1017 (proposed Site CA-9D) by 0815 hr on 19 May.

SITE 1017 (PROPOSED SITE CA-9D)

Transit from Site 1016 to Site 1017

The 58.0-nmi transit from Site 1016 to Site 1017 (proposed Site CA-9D) was accomplished in 5.25 hr at an average speed of 11.2 kt. The *JOIDES Resolution* arrived at Site 1017 at 1330 hr on 19 May.

Hole 1017A

Hole 1017A was spudded at 1615 hr on 19 May. Core 167-1017A-1H was taken from 0 to 9.5 mbsf with 100% recovery. A full barrel prevented the establishment of an accurate mudline and the hole was abandoned.

Hole 1017B

The drill pipe was raised 5 m, and Hole 1017B was spudded at 1645 hr on 19 May. APC Cores 167-1017B-1H through 13H were taken from 0 to 119.1 mbsf with 96.7% recovery.

Adara temperature measurements were taken on Cores 4H, 6H, and 8H. While extracting the core liner following Core 13H, the lower end of the liner fragmented. Safety procedures for handling overpressurized core liners were in place, and no injuries occurred. XCB Cores 167-1017B-14X through 23X were taken down to 204.2 mbsf with 92.4% recovery.

Hole 1017C

The vessel was offset 10 m to the west and Hole 1017C was spudded at 1045 hr on 20 May. APC Cores 167-1017C-1H through 8H were taken from 0 to 73.8 mbsf with 105.2% recovery. Oriented cores were obtained starting with Core 3H. XCB Cores 167-1017C-9X through 19X were taken down to 174.3 mbsf 97.2% recovery. While retrieving Core 14X, the sinker bars hit the crown sheave, parting the coring line. The sinker bars and the oil saver fell to the rig floor. No injuries occurred as a result of this incident, but additional safety equipment was installed on the coring winch unit. The winch unit now comes to a complete stop automatically at 10 mbrf and must be reset to continue advancing upward. Coring resumed with the forward coring line.

Hole 1017D

The vessel was offset 10 m to the west, and Hole 1017D was spudded at 0045 hr on 21 May. APC Cores 1017D-1H through 9H were taken down to 80.1 mbsf with 105.7% recovery. XCB Cores 167-1017D-10X through 12X were taken down to 107.9 mbsf with 78.8% recovery.

Hole 1017E

The vessel was offset 10 m to the west, and Hole 1017E was spudded at 0945 hr on 21 May. APC Cores 167-1017E-1H through 3H were taken down to 24.9 mbsf with 103.3% recovery. The drill string was tripped back to the surface and secured for the 18-hr transit to Site 1018 (proposed Site CA-8A) by 1330 hr on 21 May.

SITE 1018 (PROPOSED SITE CA-8A)

Transit from Site 1017 to Site 1018

The 180.0-nmi transit from Site 1017 to Site 1018 was accomplished in 18.5 hr at an average speed of 9.7 kt. A 3.5-kHz PDR survey was performed while approaching Site 1018. The *JOIDES Resolution* arrived at Site 1018 at 0815 hr on 22 May.

Hole 1018A

Site 1018 is located approximately 6 nmi outside an area marked "Explosive Dumping Area Disused". A subsea camera survey of the seafloor was conducted within a 50-m perimeter of the coordinates for Site 1018. One object with approximately the size and shape of a 55-gallon drum was found approximately 50 m south of Site 1018. The vessel was offset 100 m to the northeast of the Site 1018 coordinates, or 150 m from the object. The results of the camera survey at the new position were negative. Hole 1018A was spudded at 1830 hr 22 May. APC Cores 167-1018A-1H through 10H were taken down to 90.4 mbsf with 104.4% recovery. Cores 1H and 2H were run through the MST, and then split open to search for artifacts. The search results were negative. Adara temperature measurements were taken on Cores 4H, 6H, 8H, and 10H. XCB Cores 167-1018A-11X through 45X were taken down to 426.2 mbsf with 99.0% recovery. A 30-barrel sepiolite mud pill was circulated, and a wiper trip was performed in preparation for logging. Hole 1018A was logged with the Triple Combination. The logging tool string would not pass below 225 mbsf, and was run from 225 to 80 mbsf. The logging tools were rigged down and another wiper trip to bottom was made. The Triple Combination was run from 341 to 232 mbsf. The caliper log indicated a large hole diameter, and further logs were canceled.

Hole 1018B

Hole 1018B was spudded at 1530 hr on 23 May. APC Cores 167-1018B-1H through 2H were taken from 0 to 19.2 mbsf with 101.3% recovery.

Hole 1018C

Hole 1018C was spudded at 1645 hr on 23 May. APC Cores 167-1018C-1H through 10H were taken down to 88.5 mbsf with 104.3% recovery. Oriented cores were obtained starting with Core 3H. XCB Cores 167-1018C-11X through 28X were taken down to 262.2 mbsf with 97.6% recovery.

Hole 1018D

The vessel was offset 10 m to the west, and Hole 1018D was spudded at 1700 hr on 26 May. APC Cores 167-1018D-1H through 11H were taken from 0 to 104.3 mbsf with 101.5% recovery. XCB Cores 167-1018D-12X through 18X were taken down to 167.7 mbsf with 96.9% recovery. The drill string was tripped back to the surface and secured for the 48-hr transit to Site 1019 by 1130 hr on 27 May.

SITE 1019 (PROPOSED SITE CA-1D)

Transit from Site 1018 to Site 1019

The 298.0-nmi transit from Site 1018 to Site 1019 (proposed Site CA-1D) was accomplished in 43.25 hr at an average speed of 6.8 kt. The transit was made in the face of a gale force 8 storm with 16- to 18-ft seas and against a prevailing 3-kt current. A 3.5-kHz PDR survey was performed while approaching Site 1019. The *JOIDES Resolution* arrived at Site 1019 at 0730 hr on 29 May.

Hole 1019A

Hole 1019A was spudded at 1100 hr on 29 May. A full barrel prevented the establishment of an accurate mudline, and the hole was abandoned.

Hole 1019B

Hole 1019B was spudded at 1145 hr on 29 May. Again, a full barrel prevented the estab-

lishment of an accurate mudline, and the hole was abandoned.

Hole 1019C

Hole 1019C was spudded at 1230 hr on 29 May. APC Cores 167-1019C-1H through 8H were taken down to 74.8 mbsf with 107.1% recovery. Adara temperature measurements were taken on Cores 4H, 6H, and 8H. The temperature profile was linear, with a gradient of 0.057˚C/m. XCB Cores 167-1019C-9X through 26X were taken down to 247.8 mbsf with 77.4% recovery. Gas expansion caused significant gaps in the core, resulting in less than 100% core recovery. The gas was biogenic in origin and consisted mainly of methane. A 20-barrel sepiolite mud pill was circulated and a wiper trip was performed in preparation for logging. Hole 1019C was logged with the Triple Combination, FMS/Sonic, and GHMT tool strings.

Hole 1019D

The vessel was offset 10 m south, and Hole 1019D was spudded at 0245 hr on 31 May. APC Cores 167-1019D-1H through 7H were taken down to 60.6 mbsf with 101.3% recovery. Oriented cores were obtained starting with Core 3H. XCB Cores 167-1019D-8X through 24X were taken down to 223.8 mbsf with 74.5% recovery. The reduced core recovery was caused by gas expansion similar to Hole 1019C.

Hole 1019E

The vessel was offset 10 m south, and Hole 1019E was spudded at 2145 hr 31 May. APC Cores 167-1019E-1H through 12H were taken down to 109.5 mbsf with 102.4% recovery. The drill string was tripped back to the surface and secured for the 8-hr transit to Site 1020 by 0730 hr on 1 June.

SITE 1020 (PROPOSED SITE CA-4A)

Transit from Site 1019 to Site 1020

The 79.0-nmi transit from Site 1019 to Site 1020 (proposed Site CA-4A) was accomplished in 7.0 hr at an average speed of 10.9 kt. A 3.5-kHz PDR survey was performed while approaching Site 1020. The *JOIDES Resolution* arrived at Site 1020 at 1445 hr on 1 June.

Hole 1020A

Hole 1020A was spudded at 2030 hr 1 June. A full barrel prevented the establishment of an accurate mudline, and the hole was abandoned.

Hole 1020B

The drill string was raised 5 m and Hole 1020B was spudded at 2115 hr on 1 June. APC Cores 167-1020B-1H through 18H were taken down to 169.3 mbsf with 105.1% recovery. Adara temperature measurements were taken on Cores 4H, 6H, and 8H. Oriented cores were obtained starting with Core 3H. XCB Cores 167-1020B-19X through 30X were taken down to 278.8 mbsf with 79.5% recovery. Hole 1020B was logged with the Triple Combination, FMS/Sonic, and GHMT strings with excellent results.

Hole 1020C

The vessel was offset 10 m to the south, and Hole 1020C was spudded at 0545 hr on 4 June. APC Cores 167-1020C-1H through 16H were taken down to 146.8 mbsf with 104.0% recovery. Oriented cores were obtained again starting with Core 3H. XCB Cores 167-1020C-17X through 25X were taken down to 233.2 mbsf with 100.5% recovery.

Hole 1020D

The vessel was offset 10 m to the south and Hole 1020D was spudded at 0715 hr on 5 June. APC Cores 167-1020D-1H through 17H were taken down to 156.2 mbsf with 104.8% recovery. The drill string was tripped back to the surface and secured for the 12-hr transit to Site 1021 by 0130 hr on 6 June.

SITE 1021 (PROPOSED SITE CA-5A)

Transit from Site 1020 to Site 1021

The 131.0-nmi transit from Site 1020 to Site 1021 (proposed Site CA-5A) was accomplished in 11.75 hr at an average speed of 10.9 kt. A 3.5-kHz PDR survey was performed while approaching Site 1021. The *JOIDES Resolution* arrived at Site 1021 at 1315 hr on 6 June.

Hole 1021A

Hole 1021A was spudded at 2000 hr on 6 June. A full barrel prevented the establishment of an accurate mudline, and the hole was abandoned.

Hole 1021B

Hole 1021B was spudded at 2100 hr on 6 June. APC Cores 167-1021B-1H through 18H were taken down to 169.5 mbsf with 104.6% recovery. Adara temperature measurements were taken on Cores 4H, 6H, and 8H. Oriented cores were obtained starting with Core 3H. XCB Cores 167-1021B-19X through 33X were taken down to 310.1 mbsf with 96.1% recovery.

Hole 1021C

The vessel was offset 10 m to the south, and Hole 1021C was spudded at 1545 hr on 8 June. APC Cores 167-1021C-1H through 18H were taken down to 164.1 mbsf with 103.8% recovery. Oriented cores were obtained again starting with Core 3H.

Hole 1021D

The vessel was offset 10 m south, and Hole 1021D was spudded at 1330 hr on 9 June. APC Cores 167-1021D-1H through 15H were taken down to 138.5 mbsf with 103.9% recovery. The drill string was tripped back to the surface and secured for the 12-hr transit to Site 1022 by 1530 hr on 10 June.

SITE 1022 (PROPOSED SITE CA-2B)

Transit from Site 1021 to Site 1022

The 128.0-nmi transit from Site 1021 to Site 1022 (proposed Site CA-2B) was accomplished in 13.5 hr at an average speed of 9.5 kt. The *JOIDES Resolution* arrived at Site 1022 at 0500 hr on 11 June.

Hole 1022A

Hole 1022A was spudded at 1015 hr on 11 June. APC Cores 167-1022A-1H through 18H were taken down to 166.0 mbsf with 103.4% recovery. Adara temperature measurements were taken on Cores 4H, 6H, and 8H. Oriented cores were obtained starting with Core 3H.

Hole 1022B

The vessel was offset 10 m to the south, and Hole 1022B was spudded at 0215 hr on 12 June. APC Cores 167-1022B-1H through 11H were taken down to 101.2 mbsf with 105.7% recovery.

Hole 1022C

The vessel was offset 10 m to the south and Hole 1022C was spudded at 1115 hr on 12 June. APC Cores 167-1022C-1H through 17H were taken to 159.5 mbsf with 103.3% recovery. XCB Cores 167-1022C-18X through 42X were taken down to 387.7 mbsf with 93.9% recovery. Hole 1022C was logged with the Triple Combination, FMS/Sonic, and GHMT tool strings with excellent results. The drill string was tripped back to the surface and secured for the 18-hr transit to San Francisco by 1030 hr on 15 June.

OPERATIONS RESUME
LEG 167

Total Days (19 April 1996 to 16 May 1996)	58.00
Total Days in Port	1.60
Total Days Underway	12.85
Total Days on Site	43.40

	days
Coring	30.85
Tripping Time	7.49
Logging/Downhole Science	4.27
Mechanical Repair Time (Contractor)	0.18
Stuck pipe/Hole Trouble	0.15
Reentry Time	0.00
W.O.W.	0.00
Drilling	0.00
Other	0.00

Total Distance Traveled (nmi)	3102
Average Speed Transit (kt):	10.3
Number of Sites	13.0
Number of Holes	52.0
Number of Cores Attempted	840.0
Total Interval Cored (m)	7709.5
Total Core Recovery (m)	7501.5
% Core Recovery	97.30
Total Interval Drilled (m)	0.0
Total Penetration	7709.5
Maximum Penetration (m)	449.0
Minimum Penetration (m)	9.2
Maximum Water Depth (m from drilling datum)	4226.4
Minimum Water Depth (m from drilling datum)	911.9

OCEAN DRILLING PROGRAM

SITE SUMMARY

Leg 167

Hole	Latitude	Longitude	Water depth (mbrf)	Total No. cores	Interval cored (meters)	Core recov-ered (meters)	Percent recovered (percent)	Drilled (meters)	Total penetra-tion (meters)	Time on hole (hours)	Time on site (days)
1010A	29°57.9020′N	118°06.0466′W	3475.3	1	9.2	9.15	99.5%	0.0	9.2	9.00	0.4
1010B	29°57.8984′N	118°06.0436′W	3476.3	3	23.2	23.71	102.2%	0.0	23.2	4.50	0.2
1010C	29°57.9050′N	118°06.0473′W	3476.5	24	213.9	192.94	90.2%	0.0	213.9	28.50	1.2
1010D	29°57.9012′N	118°06.0387′W	3477.5	6	51.5	54.47	105.8%	0.0	51.5	12.00	0.5
1010E	29°57.9045′N	118°06.0322′W	3476.5	19	180.2	185.23	102.8%	0.0	180.2	29.25	1.2
1010F	29°57.8966′N	118°06.0337′W	3476.3	6	55.7	56.76	101.9%	0.0	55.7	11.25	0.5
1010 SITE TOTALS:				59	533.7	522.26	97.9%	0.0	533.7	94.50	3.9
1011A	31°16.8229′N	117°38.0178′W	2032.5	1	9.5	9.84	103.6%	0.0	9.5	5.50	0.2
1011B	31°16.8172′N	117°38.0080′W	2032.5	31	281.5	271.05	96.3%	0.0	281.5	43.75	1.8
1011C	31°16.8186′N	117°38.0135′W	2033.2	20	184.3	189.87	103.0%	0.0	184.3	17.75	0.7
1011D	31°16.8161′N	117°38.0189′W	2031.1	2	16.9	17.24	102.0%	0.0	16.9	1.25	0.1
1011E	31°16.8209′N	117°38.0148′W	2030.8	16	142.3	148.52	104.4%	0.0	142.3	8.75	0.4
1011 SITE TOTALS:				70	634.5	636.52	100.3%	0.0	634.5	77.00	3.2
1012A	32°16.9698′N	118°23.0243′W	1784.2	30	273.5	269.74	98.6%	0.0	273.5	30.50	1.3
1012B	32°16.9506′N	118°23.0300′W	1782.7	14	132.3	131.26	99.2%	0.0	132.3	9.75	0.4
1012C	32°16.9695′N	118°23.0391′W	1782.9	9	82.6	86.89	105.2%	0.0	82.6	9.50	0.4
1012 SITE TOTALS:				53	488.4	487.89	99.9%	0.0	488.4	49.75	2.1
1013A	32°48.0398′N	118°53.9222′W	1575.4	16	146.1	137.1	93.8%	0.0	146.1	16.00	0.7
1013B	32°48.0593′N	118°53.9271′W	1574.4	11	103.8	107.97	104.0%	0.0	103.8	7.50	0.3
1013C	32°48.0609′N	118°53.9172′W	1575.8	8	72.2	73.96	102.4%	0.0	72.2	7.25	0.3
1013 SITE TOTALS:				35	322.1	319.03	99.0%	0.0	322.1	30.75	1.3
1014A	32°49.9937′N	119°58.9031′W	1175.8	50	449.0	404.35	90.1%	0.0	449.0	61.25	2.6
1014B	32°50.0454′N	119°58.8737′W	1177.7	27	245.0	224.69	91.7%	0.0	245.0	18.00	0.8
1014C	32°50.0438′N	119°58.8811′W	1176.4	2	19.0	19.53	102.8%	0.0	19.0	1.25	0.1
1014D	32°50.0457′N	119°58.8784′W	1177.0	13	120.9	118.96	98.4%	0.0	120.9	7.75	0.3
1014 SITE TOTALS:				92	833.9	767.53	92.0%	0.0	833.9	88.25	3.7
1015A	33°42.9254′N	118°49.1852′W	911.9	16	149.5	139.12	93.1%	0.0	149.5	14.00	0.6
1015B	33°42.9213′N	118°49.1186′W	912.6	12	97.8	81.32	83.1%	0.0	97.8	9.75	0.4
1015 SITE TOTALS:				28	247.3	220.44	89.1%	0.0	247.3	23.75	1.0
1016A	34°32.3149′N	122°16.5944′W	3845.4	36	316.5	303.65	95.9%	0.0	316.5	81.50	3.4
1016B	34°32.3133′N	122°16.5772′W	3847.7	23	210.8	218.1	103.5%	0.0	210.8	26.50	1.1
1016C	34°32.2917′N	122°16.5913′W	3846.3	2	18.7	18.76	100.3%	0.0	18.7	2.25	0.1
1016D	34°32.3056′N	122°16.5851′W	3845.5	16	150.5	154.16	102.4%	0.0	150.5	19.50	0.8
1016 SITE TOTALS:				77	696.5	694.67	99.7%	0.0	696.5	129.75	5.4

Hole	Latitude	Longitude	Water depth (mbrf)	Total No. cores	Interval cored (meters)	Core recov-ered (meters)	Percent recovered (percent)	Drilled (meters)	Total penetra-tion (meters)	Time on hole (hours)	Time on site (days)
1017A	34˚32.0850′N	121˚06.4217′W	966.7	1	9.8	9.85	100.5%	0.0	9.8	3.25	0.1
1017B	34˚32.0920′N	121˚06.4145′W	966.2	23	204.2	188.74	92.4%	0.0	204.2	17.00	0.7
1017C	34˚32.0934′N	121˚06.4183′W	967.2	19	174.3	169.37	97.2%	0.0	174.3	14.25	0.6
1017D	34˚32.0904′N	121˚06.4272′W	966.4	12	107.9	85.01	78.8%	0.0	107.9	9.00	0.4
1017E	34˚32.0985′N	121˚06.4304′W	966.6	3	24.9	25.71	103.3%	0.0	24.9	4.50	0.2
1017 SITE TOTALS:				58	521.1	478.68	91.9%	0.0	521.1	48.00	2.0
1018A	36˚59.3901′N	123˚16.5332′W	2488.6	45	426.2	426.85	100.2%	0.0	426.2	78.25	3.3
1018B	36˚59.3920′N	123˚16.5323′W	2486.8	2	19.2	19.45	101.3%	0.0	19.2	2.00	0.1
1018C	36˚59.3882′N	123˚16.5375′W	2488.0	28	262.2	261.44	99.7%	0.0	262.2	23.50	1.0
1018D	36˚59.3918′N	123˚16.5438′W	2487.2	18	167.7	167.35	99.8%	0.0	167.7	18.50	0.8
1018 SITE TOTALS:				93	875.3	875.09	100.0%	0.0	875.3	122.25	5.1
1019A	41˚40.9686′N	124˚55.9804′W	991.4	1	10.1	10.11	100.1%	0.0	10.1	4.25	0.2
1019B	41˚40.9764′N	124˚55.9827′W	995.4	1	10.1	10.08	99.8%	0.0	10.1	0.75	0.0
1019C	41˚40.9723′N	124˚55.9758′W	988.2	26	247.8	213.97	86.3%	0.0	247.8	37.25	1.6
1019D	41˚40.9685′N	124˚55.9790′W	988.9	24	223.8	183.03	81.8%	0.0	223.8	19.25	0.8
1019E	41˚40.9634′N	124˚55.9793′W	989.5	12	109.5	112.17	102.4%	0.0	109.5	10.50	0.4
1019 SITE TOTALS:				64	601.3	529.36	88.0%	0.0	601.3	72.00	3.0
1020A	41˚00.5090′N	126˚26.0654′W	3052.9	1	10	10.02	100.2%	0.0	10.0	6.50	0.3
1020B	41˚00.5101′N	126˚26.0642′W	3050.1	30	278.8	265	95.1%	0.0	278.8	54.00	2.3
1020C	41˚00.5051′N	126˚26.0631′W	3049.2	25	233.2	239.49	102.7%	0.0	233.2	26.75	1.1
1020D	41˚00.5011′N	126˚26.0671′W	3049.1	17	156.2	163.74	104.8%	0.0	156.2	19.50	0.8
1020 SITE TOTALS:				73	678.2	678.25	100.0%	0.0	678.2	106.75	4.4
1021A	39˚05.2498′N	127˚46.9926′W	4226.4	1	9.5	9.86	103.8%	0.0	9.5	7.75	0.3
1021B	39˚05.2476′N	127˚46.9848′W	4222.9	33	310.2	311.62	100.5%	0.0	310.2	41.75	1.7
1021C	39˚05.2462′N	127˚46.9815′W	4224.3	18	164.1	170.39	103.8%	0.0	164.1	21.75	0.9
1021D	39˚05.2401′N	127˚46.9833′W	4223.8	15	138.5	143.84	103.9%	0.0	138.5	27.00	1.1
1021 SITE TOTALS:				67	622.3	635.71	102.2%	0.0	622.3	98.25	4.1
1022A	40˚04.8506′N	125˚20.5588′W	1938.4	18	166.0	171.57	103.4%	0.0	166.0	19.00	0.8
1022B	40˚04.8500′N	125˚20.5614′W	1937.3	11	101.2	105.69	104.4%	0.0	101.2	10.25	0.4
1022C	40˚04.8417′N	125˚20.5580′W	1937.5	42	387.7	378.85	97.7%	0.0	387.7	71.25	3.0
1022 SITE TOTALS:				71	654.9	656.11	100.2%	0.0	654.9	100.50	4.2
LEG 167 TOTALS:				840	7709.5	7501.54	97.3%	0.0	7709.5	1041.5	43.4

LEG 167
ON-SITE TIME DISTRIBUTION

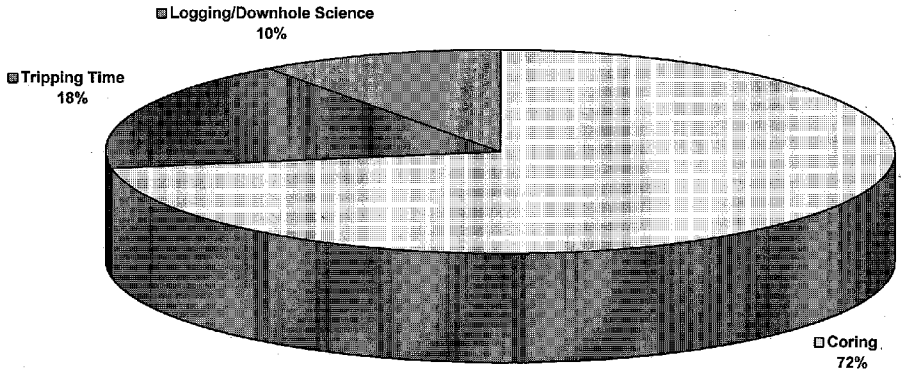

ALL OTHER CATEGORIES < 1 %

LEG 167
TOTAL TIME DISTRIBUTION

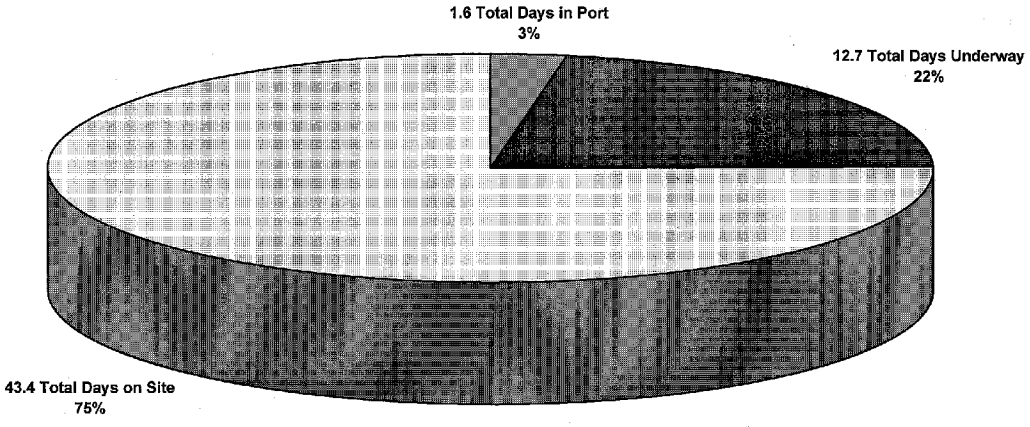

Total days of leg = 57.9

TECHNICAL REPORT

The ODP Technical and Logistics personnel aboard *JOIDES Resolution* for Leg 167 were:

John DykeMarine Lab Specialist (Store Keeper)

John EastlundMarine Computer Specialist

Tim FultonMarine Lab Specialist (Photographer)

Edwin GarrettMarine Lab Specialist (Paleomagnetics)

Dennis GrahamMarine Lab Specialist (Chemistry)

Thilo GrebMarine Lab Specialist

Michiko HitchcoxMarine Lab Specialist (Yeoperson)

Rich JohnsonMarine Computer Specialist

Brad JulsonLaboratory Officer

John LeeMarine Lab Specialist (Chemistry)

Kevin MacKillopMarine Lab Specialist (Physical Properties)

Eric MeissnerMarine Electronics Specialist

Dwight MossmanMarine Electronics Specialist

Chieh PengMarine Lab Specialist (Chemistry)

Thomas PollaertMarine Lab Specialist

Rebecca RobinsonMarine Lab Specialist

Don SimsMarine Lab Specialist (X-ray)

Lorraine SoutheyMarine Lab Specialist (Curatorial)

Joel SparksMarine Lab Specialist (X-ray)

Nancy SmithMarine Lab Specialist (Curatorial)

GENERAL LEG INFORMATION

Leg 167 drilled 52 holes at 13 sites and recovered over 7500 m of core. This is a new ODP core recovery record. Leg 167 officially began on April 20 in Acapulco, Mexico. Many of the technical staff boarded the ship 10 days earlier in Panama for the transit to Acapulco. The transit was mainly devoted to the development and testing of the data models for the JANUS database. Most of the TRACOR development staff, the JANUS Steering Committee, and the technical staff met daily to developed the data models. The ship arrived in Acapulco in the afternoon on 19 April, 1996. The crew arrived on the ship the morning of the 20 April, and the ship sailed that afternoon. Two Mexican observers also sailed from Acapulco. Transit to the first site off Northern Baja, Mexico, took 4 days. A port call in San Diego was scheduled on the morning of 7 May to unload over 200 boxes of core to alleviate the anticipated core storage problems in the refrigerators from the expected deluge of core. One of the Mexican observers was replaced by a second curatorial representative. The ship received a shipment of fresh fruits and vegetables, and left the afternoon of the same day for the 8-hr transit to the next site. The ship slowly worked its way up the coast, drilling 13sites. A rendezvous with a small boat from the University of California, Santa Barbara (UCSB), occurred in the Santa Barbara channel on 12 May. The rendezvous allowed 5 small boxes of core to be sent to UCSB for immediate isotope analysis and biostratigraphy studies. The leg ended as the ship pulled into San Francisco on 16 June, 1996.

Port call (Acapulco)

All the oncoming shipments were loaded in Panama, and cores and samples from the previous leg were offloaded. During the transit, the saws and drill presses on the bench on the aft bulkhead in the core laboratory were removed to install the color reflectance track and system. A digital image track and system was installed on the starboard bench. The TRACOR JANUS development team sailed along with members of the JANUS Steering Committee during the transit. There were intense meetings trying to define the data models for the laboratories. Other existing data-entry screens were tested and modified as necessary.

Underway geophysics

Routine 3.5-and 12-kHz precision depth recorder (PDR) and magnetometer data were collected on all surveys. Seismic data were not collected this leg because of the excellent seismic data already existing for these sites and the slipping of the schedule

Core laboratory

During the transit, two people sailed from Oregon State University and installed the color reflectance track and system. The saws and drill presses were removed from the bench in the aft end of the core laboratory because they were not expected to be needed in the soft APC/XCB sediments. The color reflectance system was set up on this bench. Also, a digital imaging track and system was installed during the transit on the starboard bench in the core laboratory.

Core flow through the laboratory was intricate and choreographed. After the whole-round cores went through the MST track, the cores were split. The archive half of the core was scraped, run through the color reflectance system, the cryomagnetometer, and finally the digital imaging system before being described, photographed, and archived. Working halves were analyzed for velocity measurements before being sampled and finally packed away.

Paleomagnetism laboratory

There was very little time to spend on projects in the paleomagnetism laboratory. Fortunately all of the equipment worked well during the leg. About 1500 sections were run through the magnetometer. The Tensor orientation tool was run at every site, and it was run on two holes at Site 1020. This was also anticipated as the last leg for the current cryogenic magnetometer, which will be replaced at the end of the leg.

Chemistry laboratory

A total of 218 interstitial water samples were tested for salinity, alkalinity, pH, and major-element geochemistry. Headspace gas was measured for safety and pollution prevention purposes. A new method of taking vacutainer gas samples was successfully employed, using 50-ml syringes and small, three-way, stopcock valves. This method saves time, yields more sample volume, and allows more control of samples than previous methods. Lipids and high-molecular-weight hydrocarbons were extracted and measured. Large numbers of carbonate tests were run on the coulometer and CNS tests on the Carlo Erba elemental analyzer for inorganic and organic carbon. Total organic carbon, Tmax, S1, S2, and S3 were measured using the Rock-Eval.

X-ray laboratory

A total of 192 sediment samples were analyzed by X-ray diffraction (XRD). These were all simple bulk-mineral identifications in which no special preparation was required. Based on XRD results, 99% of all analyzed samples consisted of varying proportions of quartz, calcite, plagioclase, clays, and minor sulfide minerals. Dolomite, barite, and opal were occasionally identified. The X-ray fluorescence (XRF) unit was not used.

LABORATORY STATISTICS: LEG 167

General statistics:

Sites....13
Holes.... 52
Cored Interval (m)....7,709.50
Core Recovered (m)....7,501.54
Percent Recovered.... 97.30
Total Penetration (m)....7,709.50
Time on Site (days).... 43.44
Number of Cores.... 840
Number of Samples.... 22,812
Whole Rounds....243
Boxes of Core.... 1,088

Samples analyzed:

Inorganic Carbon ($CaCO_3$)....1624
Total Carbon (NCHS)....1624
Water Chemistry (the suite includes pH, Alkalinity, Sulfate, Calcium, Magnesium, Chlorinity, Potassium, Silica, Salinity)....218
Pyrolysis Evaluation (Rock Eval and GHM)....100
Gas Samples.... 513
Extractions....63
Thin Sections.... 8
XRF.... 0
XRD....200
MST Runs....5,389
Cryomagnetometer Runs....1,220
Cubes....214

Oriented Cores.....55

Physical Properties Velocity..... 423

Thermal Conductivity..... 380

Index Properties.....2,184

Resistivity:.....0

Shear Strength:.....0

UnderWay geophysics:

Bathymetry (nmi).....2,958

Seismic Survey (nmi).....0

XBTs launched.....48

DownHole tools:

WSTP.....0

Adara..... 44

Additional:

Close-up Photographs:.....120

Whole Core Photographs:.....822

Rolls of Photomicrographs.....0

Color Transparencies..... 822

Black-and-White Prints.....3233